Tennessee Valley Authority
Division of Water Resources
Water Systems Development Branch

MODEL STUDY AND ANALYSIS OF

SEQUOYAH NUCLEAR PLANT SUBMERGED MULTIPORT DIFFUSER

Report No. WR28-1-45-103

Prepared by
Lance N. McCold
Norris, Tennessee
March 1979

CONTENTS

	Page
Abstract	ii
List of Figures	iii
List of Tables	iv
I. Introduction	1
II. Site and Plant Characteristics	3
Site Characteristics	3
Local Hydrography	3
Stream Flow	3
Temperatures	6
Plant Characteristics	9
Heat Dissipation	9
Diffuser Discharge Temperature	9
III. Discharge Control Considerations	11
Applicable Water Quality Standards	11
Existing Diffuser and Control Elements	11
IV. Analysis	15
V. Physical Model Study	27
Simlitude Requirements	27
Description of Physical Model	30
Instrumentation	32
Model Test Program	34
Data Acquisition and Reduction Procedure	34
VI. Results	36
General Features	36
Comparison to Theory	40
Conclusions	46
References	47
Appendix	48

ABSTRACT

This report describes the analytical and physical model studies of the Sequoyah Nuclear Plant submerged multiport diffuser. The purpose of the analytical and physical model studies was to determine the dilution achieved by the Sequoyah diffuser. In the analysis, a quasi-empirical theory is developed to describe diffuser performance over a wide range of discharge parameters. The analysis is based on examinations of the governing momentum and volume length scales of the discharge and receiving water. The behavior of the diffuser plume for all buoyancies is deduced by considering the asymptotic cases of a pure jet and a pure plume.

The physical model, built to a scale of 1:90, was used to evaluate the empirical coefficients. Particular attention was paid to the near-field structure of the effluent plume. Adequate agreement with the theory was achieved over the range of conditions tested.

LIST OF TABLES

No.	Title	Page
1	Duration of Zero-Flow Periods Per Year at Watts Bar and Chickamauga Dams	7
2	Summary of Entrainment Formulae	26

I. INTRODUCTION

The Sequoyah Nuclear Plant (SNP) is being built by the Tennessee Valley Authority (TVA) on the right bank of Chickamauga Reservoir, Tennessee River Mile (TRM) 484.5. The plant is about 18 miles (29 kilometers) northeast of Chattanooga, Tennessee, and about 13 miles (21 kilometers) upstream of Chickamauga Dam (Figure 1.1). The two unit Sequoyah Nuclear Plant will have a net generating capacity of 2440 Mw_e, and an associated waste heat load of 4800 Mw_t, or 16.4×10^9 Btu/hr. The heat transferred from the steam condensers to the cooling water will be dissipated either to the atmosphere by way of two natural draft cooling towers, to the river through a two leg submerged multi-port diffuser (hereafter called the diffuser), or by a combination of both.

The discharge from the diffuser is subject to applicable Federal and State of Tennessee water quality criteria, including temperature standards. The diffuser was designed and built to meet somewhat less stringent temperature standards than are presently applicable. As a result of the more stringent temperature standards it was necessary to incorporate two natural draft cooling towers into the plant to assure sufficient cooling under all environmental conditions. In order to operate the plant as economically as possible while complying with the applicable water temperature standards, it is necessary to know how the diffuser performs under the various off-design conditions which are expected to occur. A physical model study of the SNP diffuser under a suitably wide range of conditions has been conducted by the Water Systems Development Branch of TVA. This report summarizes the methods and results of that physical model study of the SNP diffuser.

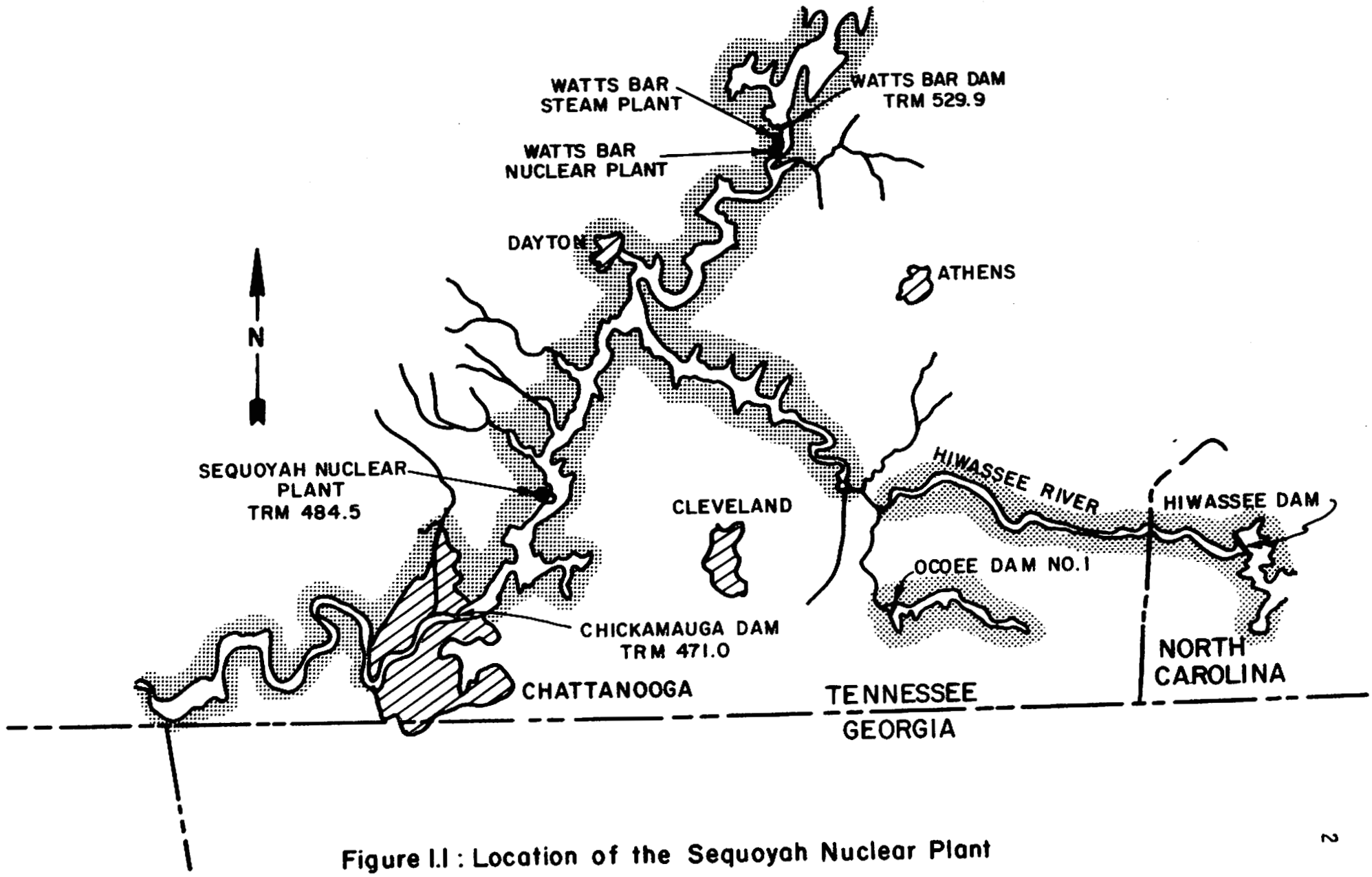

Figure I.I : Location of the Sequoyah Nuclear Plant

II. SITE AND PLANT CHARACTERISTICS

Site Characteristics

Pertinent information about the hydrography of the Tennessee River at the Sequoyah site is given below. A more detailed discussion can be found in Reference 1.

Local Hydrography

A general view of the diffuser and underwater dam locations is shown in Figure 2.1. The plant is located on the inside of a bend to the right at about TRM 484.5. In this region the Tennessee River is impounded by Chickamauga Dam (TRM 471). The reservoir in the vicinity of SNP could be characterized as a roughly rectangular main channel approximately 900 feet (274 meters) wide and 50 to 60 feet (15 to 18 meters) deep, depending on the pool elevation, with extensive and highly irregular overbank areas which are usually less than 20 feet (6.1 meters) deep (Figure 2.2). The diffuser (TRM 483.65) and the underwater dam (TRM 483.85) are the only significant obstructions in the main channel. Representative cross-sections of the main channel in the vicinity of the diffuser are shown in Figure 2.2.

Stream Flow

River flows in the vicinity of Sequoyah Nuclear Plant are controlled by releases from Chickamauga Dam (TRM 471.0), Watts Bar Dam (TRM 529.9) and to a lesser extent by the Hiwassee River (TRM 499). Daily average discharges at Chickamauga Dam have ranged from a maximum of 219,000 ft^3/sec (6200 m^3/sec) to a minimum of 700 ft^3/sec

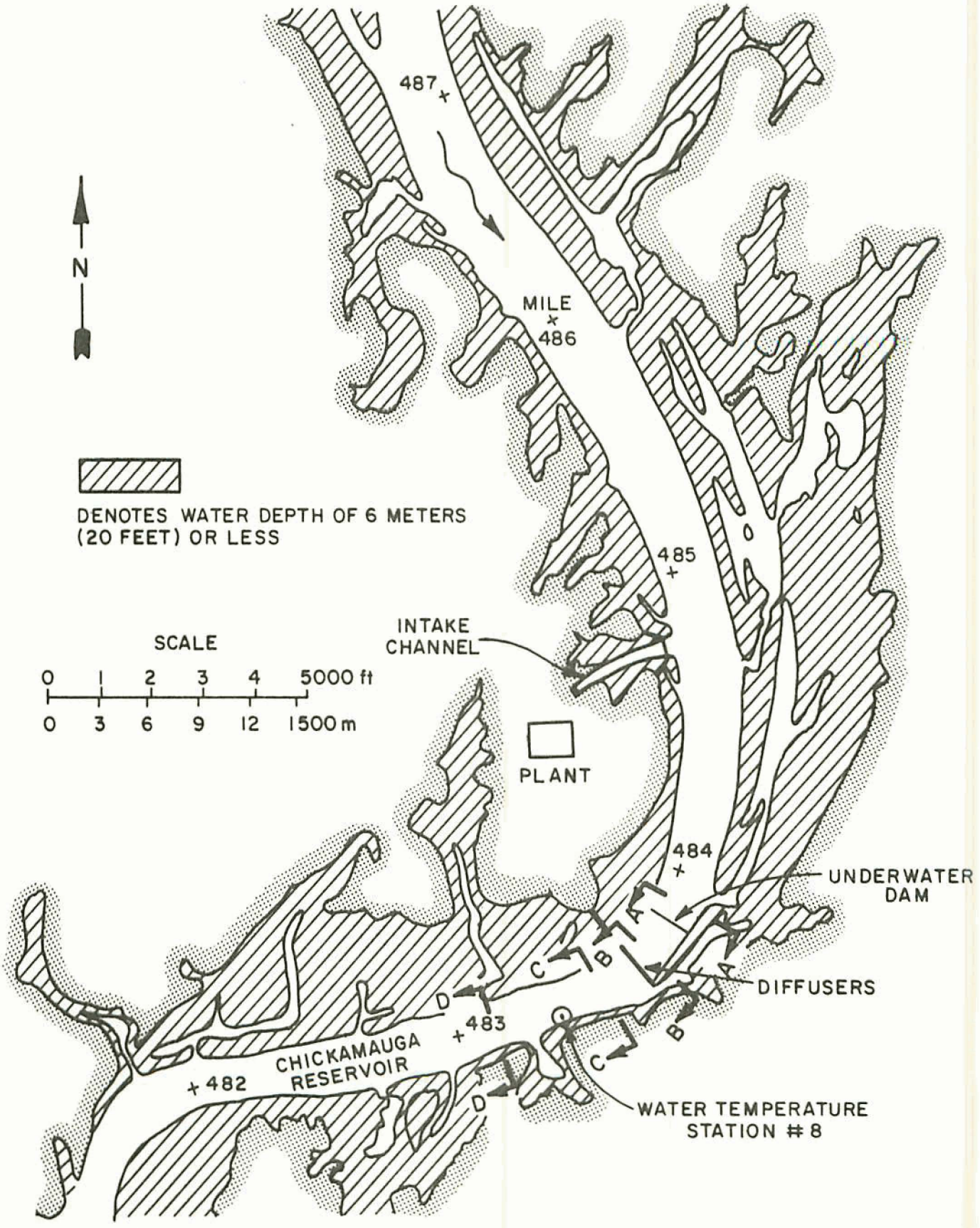

Figure 2.1: Underwater Topography Near Sequoyah Nuclear Plant

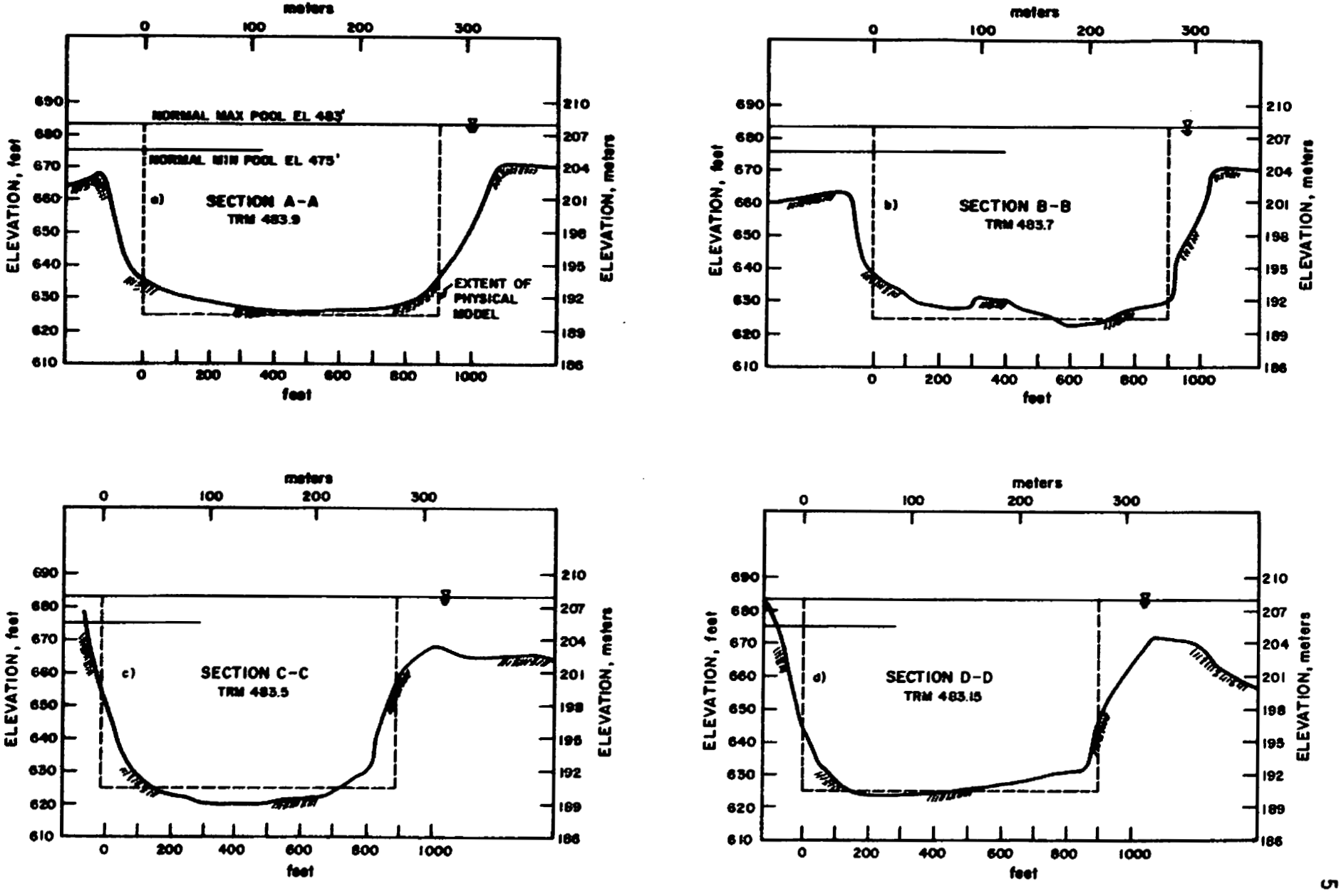

Figure 2.2 : Cross-Sections

(20 m^3/sec). At present TVA attempts to maintain a daily average discharge of 6,000 ft^3/sec (170 m^3/sec).

As is usual with dams in the Tennessee Valley system, most of the water passing the dams is used to generate electricity during peak demand periods. As a result the dam releases and river flows are highly variable over the course of a day. Since the stream flow at SNP is most sensitive to the releases at Chickamauga Dam, the discharge records for Chickamauga Dam can provide a guide to the flows to be expected at SNP. Table 1 summarizes the periods of zero flow observed in previous years.

Temperatures

The natural temperatures observed in Chickamauga Reservoir at SNP are a very complex function of environmental factors. Most of the existing temperature data comes from the ten water temperature monitors which were installed in 1973 in the vicinity of SNP, Reference 1. Both the monthly average temperatures for 1973-1976 and the daily average temperatures for 1977, recorded at monitor 8, are shown in Figure 2.3 (Monitor 8 is located just downstream of the diffuser, Figure 2.1). It is worth noting that the daily temperatures are often significantly different from the monthly averages and, as noted in Reference 1, temperatures nearly as high as the maximum allowable temperature specified in Tennessee's thermal water quality standards have been recorded. Significant diurnal temperature variations are also observed in the upper layer of the reservoir, Reference 1. Due to the complexity of the natural physical processes which affect water temperatures it is likely that plant induced thermal effects will be difficult to separate from natural effects when the plant becomes operational.

Table 1: DURATION OF ZERO-FLOW PERIODS PER YEAR AT WATTS BAR AND CHICKAMAUGA DAMS* 1959-1968

Duration (hours)	Ave. No. of Occurrences Per Year	
	Watts Bar	Chickamauga
1	14.0	2.5
2	21.2	2.9
3	29.9	6.2
4	31.7	7.5
5	32.0	6.9
6	26.6	6.7
7	17.0	4.2
8	9.9	2.4
9	4.5	1.1
10 or greater	3.2	1.0

*Data reflects period of 1959-1968 as shown in Tennessee Valley Authority, "Final Environmental Statement, Sequoyah Nuclear Plant, Units 1 and 2," Chattanooga, Tennessee.

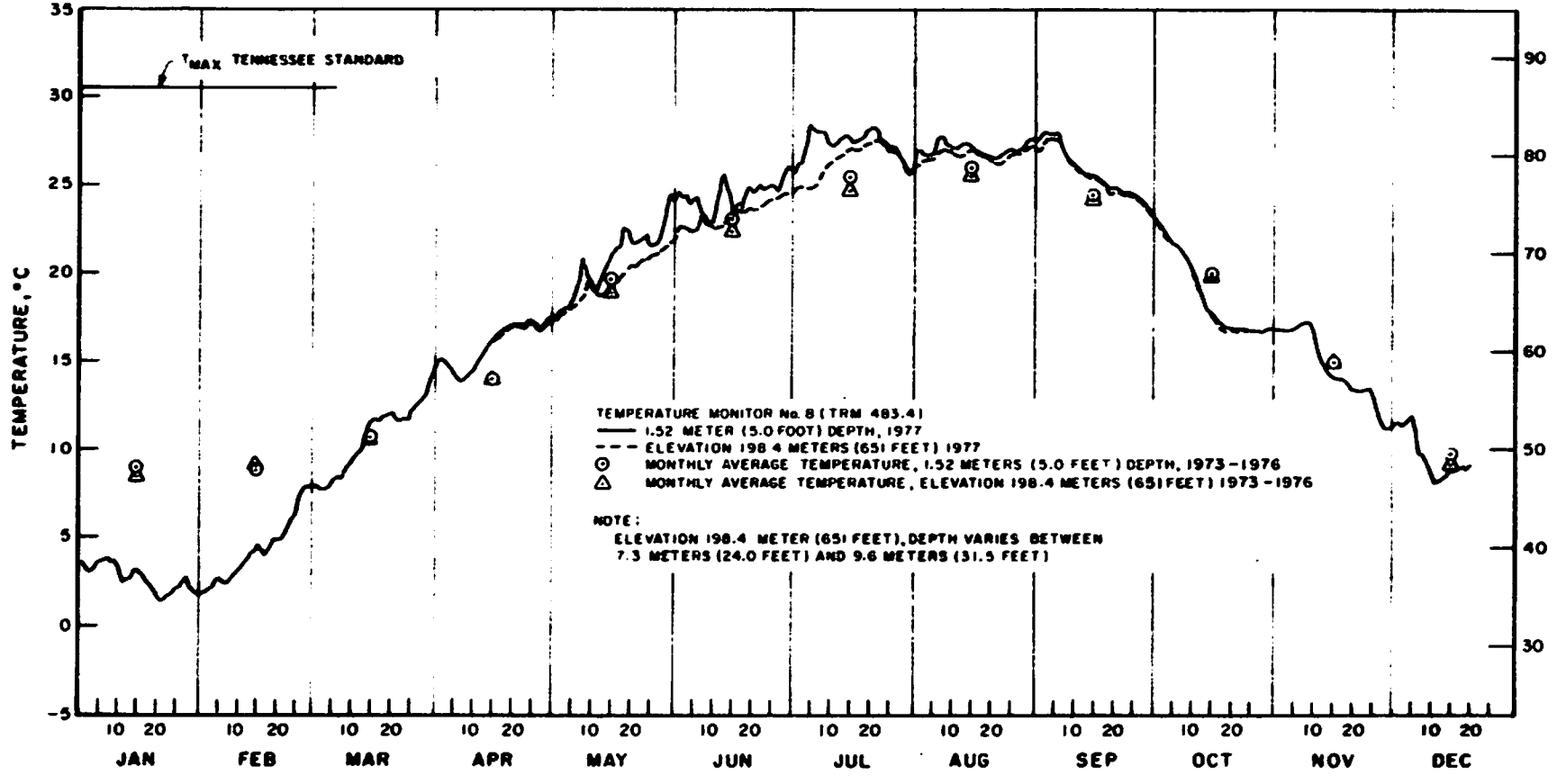

Figure 2.3: Ambient Water Temperatures in Chickamauga Reservoir Near the Sequoyah Nuclear Plant

Plant Characteristics

Heat Dissipation System

The configuration and operation of the heat dissipation system is described in detail in Reference 2. Figure 2.4 shows a plan view of the plant. The plant is designed to operate in open, closed, or helper mode. In open mode river water is pumped from the river through the plant and discharged through the diffuser. In closed mode the heated condenser cooling water discharged from the plant is pumped through the cooling towers and returned to the intake embayment via the return channel. In helper mode the heated condenser cooling water is pumped to one or both of the towers, returned to the diffuser pond and thence to the river through the diffuser.

Diffuser Discharge Temperature

The maximum thermal impact on the reservoir will occur during open mode cooling when the discharged temperatures may exceed the ambient river temperature by 29.5°F (16.4°C). Under certain atmospheric conditions it is possible to discharge water at a temperature below ambient when the cooling towers are operating; however, such a situation is not likely to occur in practice.

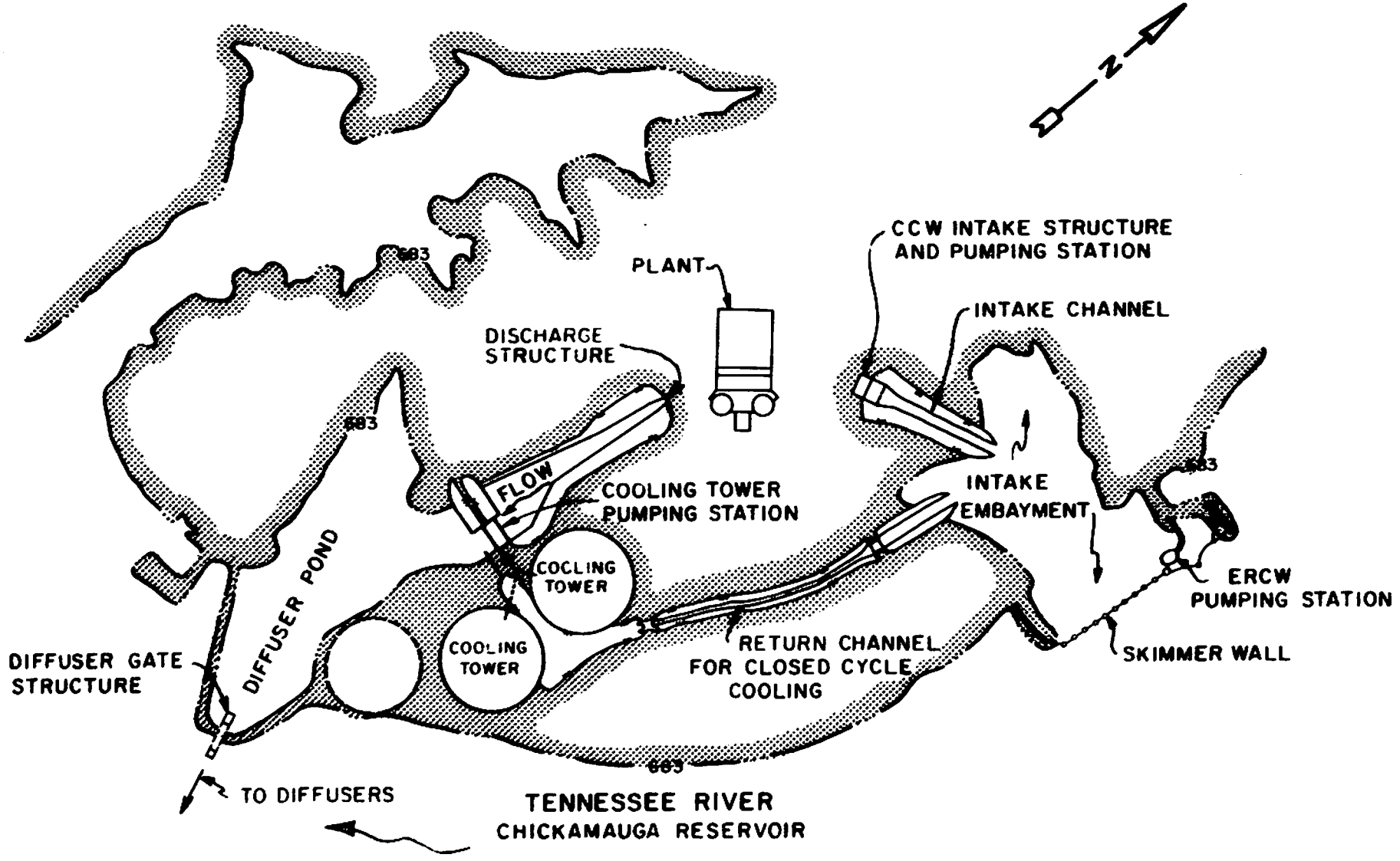

Figure 2.4: General Plan of the Sequoyah Nuclear Plant

III. DISCHARGE CONTROL CONSIDERATIONS

Applicable Water Quality Standards

Since the diffuser was designed and built, environmental standards have become more stringent. As a result cooling towers were built and several choices of cooling system operation now exist. Closed mode operation results in the least thermal impact on Chickamauga Reservoir; however, it is also the most expensive mode of cooling. To avoid these costs, as far as possible, a control program is being developed which will minimize the use of the cooling towers while meeting environmental standards. The performance of the diffuser is a crucial element of any such control program. The purpose of this study was to characterize the performance of the SNP diffuser.

The relevant water quality standards require that the plant induced temperature rise be less than 3°C (5.4°F), the maximum plant induced water temperature be 30.5°C (86.9°F) and the maximum rate of water temperature change be less than 2.0°C (3.6°F) per hour. These standards are applied outside a mixing zone which is sufficiently large that essentially all diffuser induced mixing is completed therein. For SNP the proposed mixing zone is about 750 feet (230 meters) wide and 1500 feet (460 meters) long, extending from the diffuser at TRM 483.7 downstream over the entire depth.

Existing Diffuser and Control Elements

The SNP diffuser consists of two 350 foot (107 meter) long legs. The downstream leg of the diffuser is located at the right bank of the main channel. The upstream leg begins at the end of the down-

stream leg (Figure 3.1). The water discharged through the diffuser is driven by the difference in elevation between the diffuser pond and the reservoir. The downstream leg of the diffuser is gated. The gate closes automatically when the diffuser pond elevation is less than 4 feet above the reservoir level but it must be opened manually. The upstream leg is not gated; this allows free movement of water out of or into the diffuser pond depending on the water levels in the pond and reservoir.

Located about 250 feet (80 meters) upstream of the diffuser is the underwater dam. The purpose of the dam is to retard the upstream movement of the warm water surface layer formed during low flow conditions in the reservoir. Additional details are shown in Figures 3.1 and 3.2.

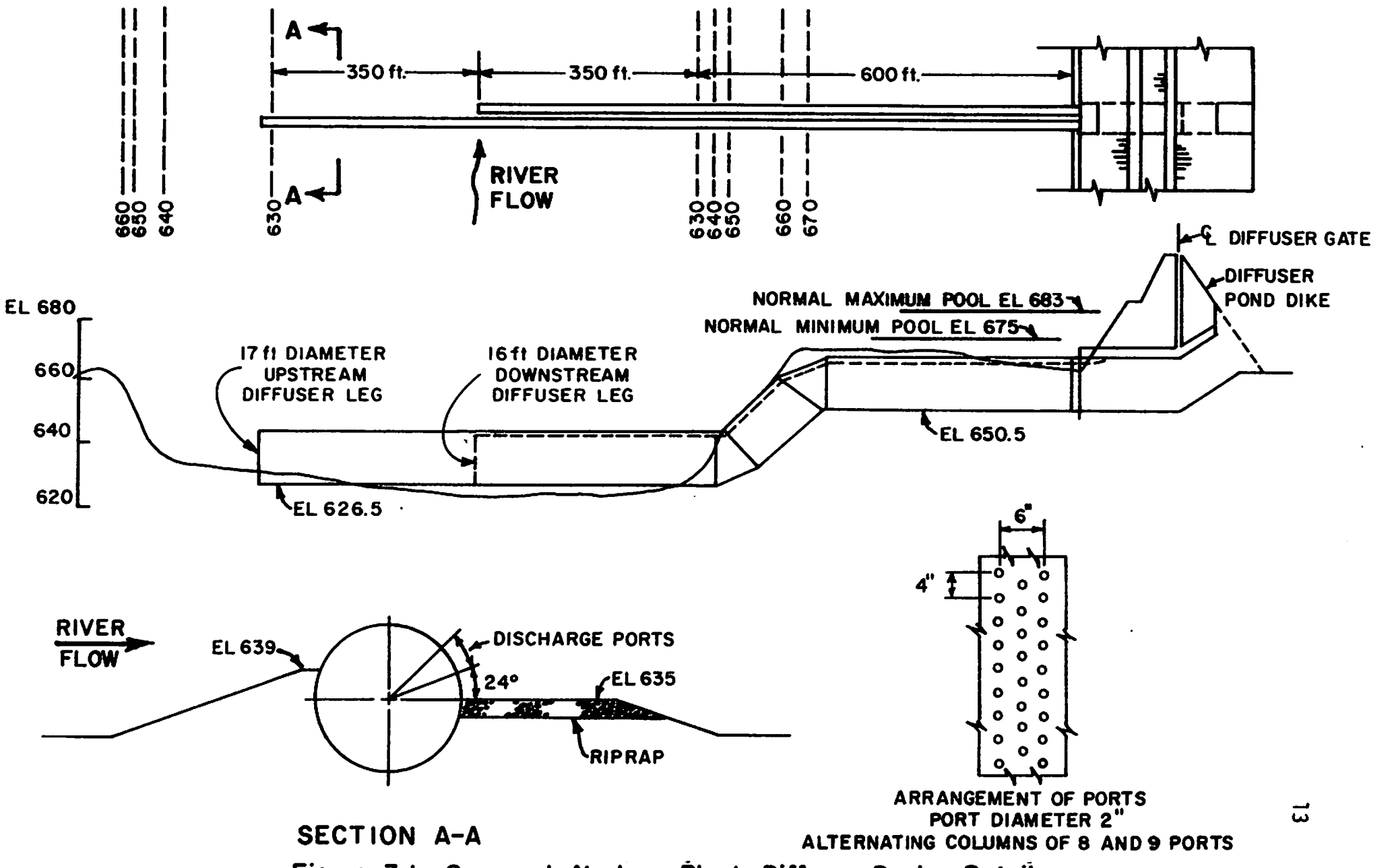

SECTION A-A

ARRANGEMENT OF PORTS
PORT DIAMETER 2"
ALTERNATING COLUMNS OF 8 AND 9 PORTS

Figure 3.1 : Sequoyah Nuclear Plant Diffuser Design Details

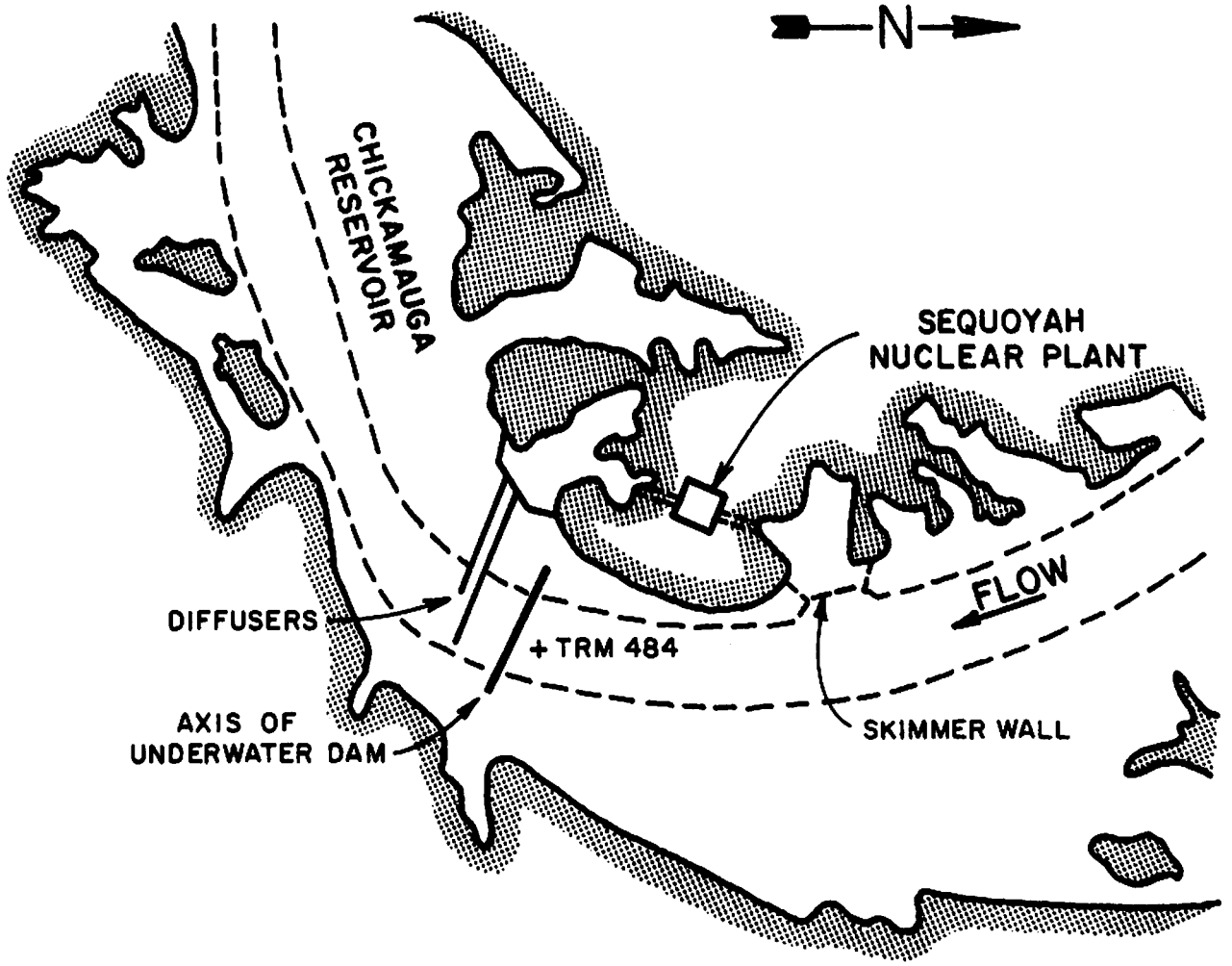

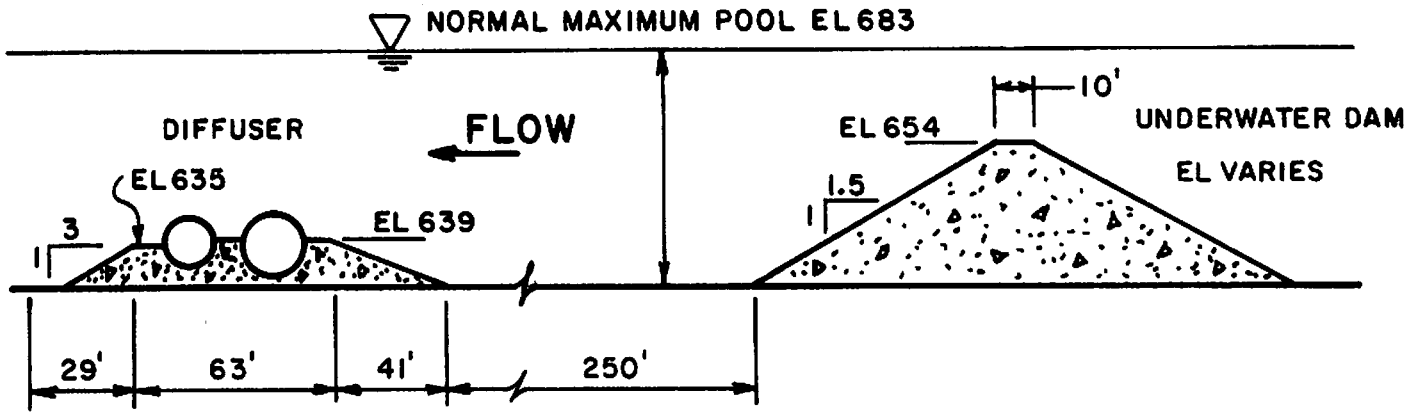

Figure 3.2: Schematic Section of Diffusers and Underwater Dam

IV. ANALYSIS

The analysis techniques used herein are essentially the same as those used in previous TVA analyses of submerged diffuser performance, Reference 3. The salient features of that analysis will be presented in this chapter.

The purpose of a diffuser is to dilute an effluent so as to reduce the possible harmful effects to organisms which come in contact with it. Dilution, S, is defined as the concentration, C_o, of a component in a sample of the undiluted fluid divided by the concentration, C, of the same component in a sample of diluted fluid. By consideration of the above definition it can be shown that for two flows which have mixed

$$S = (Q_e + Q_o)/Q_o \tag{4.1}$$

where Q_o is the flow rate of the undiluted effluent and Q_e is the flow rate of the entrained or diluting fluid. For convenience in the analysis that follows, attention will be directed to Q_e or q_e ($q_e = Q_e/L$, where L is the diffuser length) since in most cases Q_e is independent of Q_o.

Reference 3 demonstrates that for any particular diffuser geometry the performance of the diffuser is a function of three dynamic parameters. These three parameters measure the relative importance of the momentum of the diffuser discharge, the momentum of the water in the channel and the buoyancy of the discharge. The momentums and buoyancy are calculable from the known and measurable characteristics of the river and diffuser discharge.

The parameters which describe the river channel and diffuser are shown schematically in Figure 4.1. The diffuser lies perpendicular to the river channel centerline, with ports directed downstream. The river is characterized by channel width, W; depth, H; ambient temperature, T_a; and current speed, V. The diffuser is characterized by its length, L; number of ports, n; total port area, A_p; distance of the ports above the channel bottom, h; and angle of discharge with respect to horizontal, α. The discharge effluent is described by its flow rate, Q_o; and its temperature at the point of discharge, T_d.

While the mixing of heated water can be analyzed from several different viewpoints, the concern of this study is the near-field mixing region in which the overall diffuser configuration and the local receiving water conditions govern the induced mixing. Within the near-field region, three induced flow regimes may be identified. These flow regimes which are traditionally called stratified, transition and well-mixed are illustrated in Figure 4.2. In the stratified flow regime the buoyant effluent rises immediately to the surface, forming a heated flow-away layer. Cool water is entrained below this layer and may even be drawn upstream against the prevailing current. This regime will exist when the buoyancy of the discharge effluent is large enough to dominate both the discharge momentum and the river current. In the well-mixed flow regime, the heated effluent becomes uniformly mixed top to bottom for some distance downstream of the diffuser. Cool entraining water is then drawn primarily from behind the diffuser. This regime will exist when either the initial discharge momentum or the ambient water momentum are large enough to overcome the tendency of the buoyant effluent to immediately stratify. The transition regime is

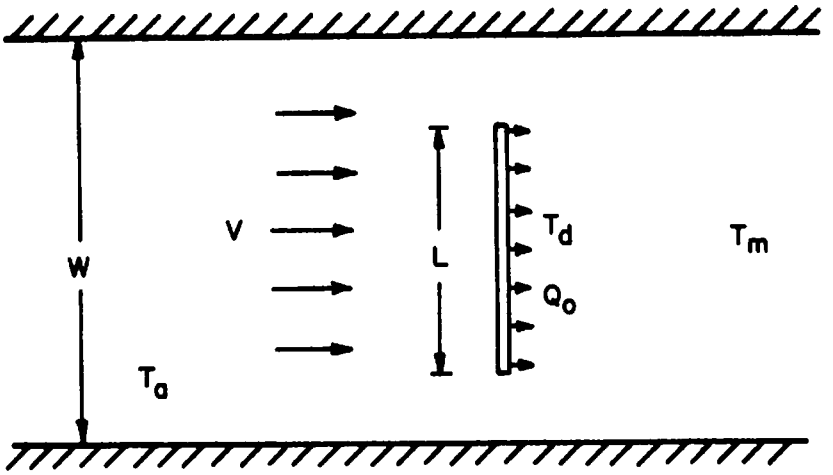

a) PLAN (not to scale)

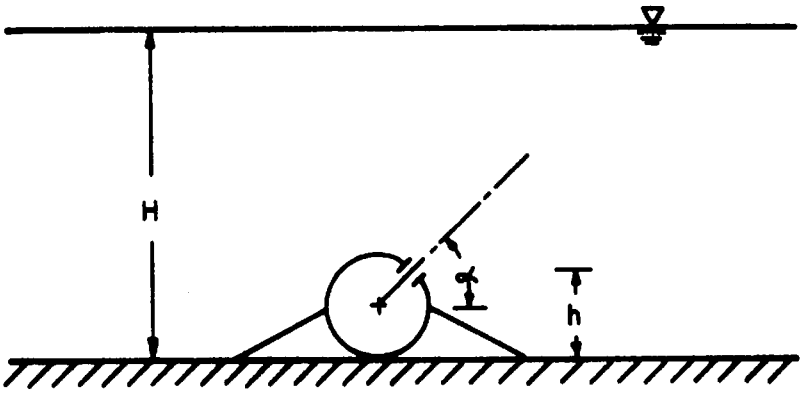

b) ELEVATION (not to scale)

Figure 4.1: Definition Sketch

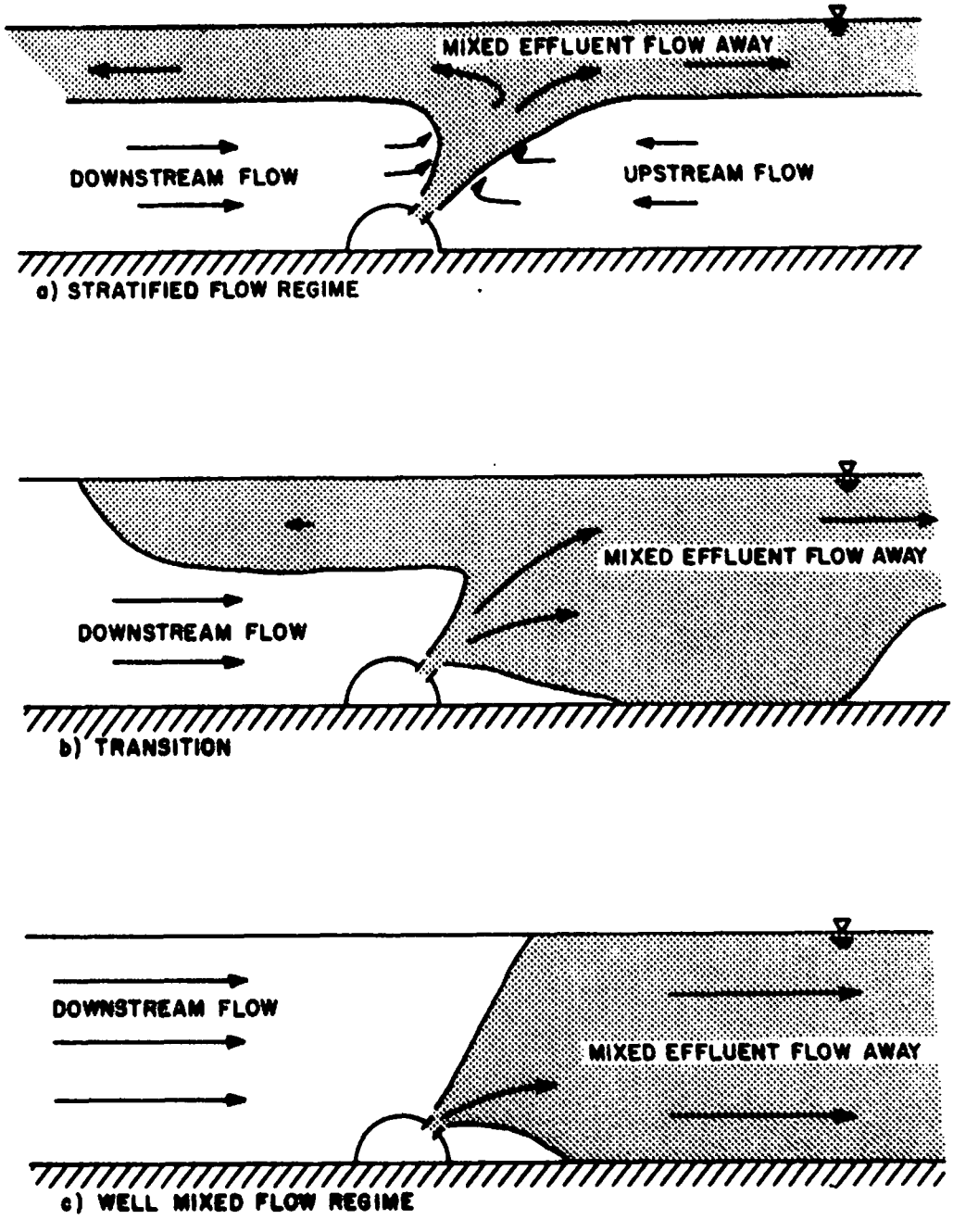

Figure 4.2 : Diffuser Flow Regimes

really a range of regimes between the extremes of the stratified and well-mixed regimes wherein discharge momentum, discharge buoyancy and ambient water momentum may all play a significant role.

In this analysis all dynamic variables are expressed in per unit mass form. This procedure allows a more streamlined formulation since it eliminates the ambient water density, ρ_a, in all but the buoyancy term. Since most of the mixing occurs in the region above and behind the diffuser all dynamic variables are also expressed in per unit diffuser length form.

The entrained volume flux per unit length is defined as

$$q_e = Q_e/L. \tag{4.2}$$

As can be seen in Equation (4.1), the larger the value of q_e achieved by a diffuser the greater the dilution. The discharged volume flux per unit length is

$$q_o = Q_o/L. \tag{4.3}$$

The volume flux, q_o, affects mixing only very near the diffuser. The discharged momentum flux per unit diffuser length is

$$m_o = Q_o^2/(A_pL). \tag{4.4}$$

The discharged buoyancy flux per unit diffuser length is

$$b_o = Q_o\ g\ (\rho_a - \rho_o)/(\rho_a L) \tag{4.5}$$

where g is the gravitational acceleration and ρ_o is the density of the discharge. The momentum length is defined as

$$\ell_m = m_o/b_o^{2/3}. \tag{4.6}$$

The momentum length is approximately the distance from the diffuser for which the discharge momentum dominates buoyancy in governing diffuser induced mixing. The river water momentum flux per unit length of diffuser is $V^2(H-h)$.

All of the parameters discussed to this point affect diffuser performance. However, for a given diffuser of fixed geometry Reference 3 shows that the diffuser performance can be expressed in non-dimensional form as

$$q_e/(m_o H)^{1/2} = f(H/\ell_m,\ V^2/b_o^{2/3}). \tag{4.7}$$

The non-dimensional form of the entrainment flow, $q_e/(m_o H)^{1/2}$, was chosen for the simplification it permits in the explicit expressions which will supplant Equation (4.7). H/ℓ_m is a parameter which is proportional to the ratio of the buoyancy induced momentum flux to the discharge momentum flux. This may be seen more clearly by using Equation (4.6) for ℓ_m;

$$H/\ell_m = H\ b_o^{2/3}/m_o. \tag{4.8}$$

The term, $V^2/b_o^{2/3}$, is proportional to the ratio of the river momentum flux which passes over the diffuser to the bouyancy induced momentum flux.

To evaluate the functional form of Equation (4.7) the solutions which already exist were examined. In the limit of a non-buoyant discharge, i.e., as $H/\ell_m \to 0$, a one-dimensional theory developed by Adams (Reference 4) for a diffuser in open water can be used to describe the diffuser performance. According to Adams' theory the diffuser induced dilution in quiescent conditions is given by

$$q_e/(m_o H)^{\frac{1}{2}} = (\cos\alpha/2)^{\frac{1}{2}} \cong 1/\sqrt{2} \tag{4.9}$$

for

$$0 < H/\ell_m < o(1) \text{ and small } \alpha.$$

For high river velocity conditions, i.e. $V/b_o^{1/3} >> o(1)$ as well as for $H\ell_m < t_m$ Adams' theory gives

$$\frac{q_{em}}{(m_o H)^{1/2}} = 1/2 \left[\frac{|V|}{b_o^{1/3}} \left(\frac{H}{\ell_m}\right)^{1/2} + \left(\frac{V^2 H}{b_o^{2/3} \ell_m} + 2 \text{ sign } (V)\right)^{1/2} \right] \tag{4.10}$$

in which sign (V) = +1 if $V \geq 0$ (forward flow) and sign (V) = -1 if $V < 0$ (reverse flow). (Note that Equation (4.10) reduces to Equation (4.9) when V = 0.)

In the limit of a very buoyant discharge, i.e. $H/\ell_m >> 1$, a pure plume theory, originally developed by Rouse (Reference 5) may be applied. The overall entrainment flow of a pure two-dimensional plume in a quiescent receiving water of infinite depth is given by Reference 6 as

$$q_e = 0.59\ b_o^{2/3}\ z \tag{4.11}$$

where z is the vertical distance above the discharge. After accounting for the finite water depth, the thickness of the buoyant flow-away layer and the depth of the diffuser ports the form of Equation (4.11) appropriate for this diffuser is

$$q_e = 0.59\ (5/6\ (H - h))\ b_o^{2/3}. \tag{4.12}$$

Since for this study H is fixed at 58 feet and h is fixed at about 15 feet Equation (4.11) may be rewritten as

$$\begin{aligned} q_e &= 0.59\ (5/6)(43/58)\ Hb_o^{2/3}, \\ &= 0.36\ Hb_o^{2/3}. \end{aligned} \tag{4.13}$$

By assuming transitions between the extreme cases discussed above Reference 3 gives a theory which is applicable to most flow regimes. The general form of the theory for quiescent river conditions is illustrated graphically in Figure 4.3. Note that the quiescent river solution consists of a momentum solution for $H/\ell_m < o(1)$, a plume solution for $H/\ell_m > o(10)$ and a transition with an intermediate slope that connects the other two solutions. The solutions for $V/b_o^{1/3}$ other

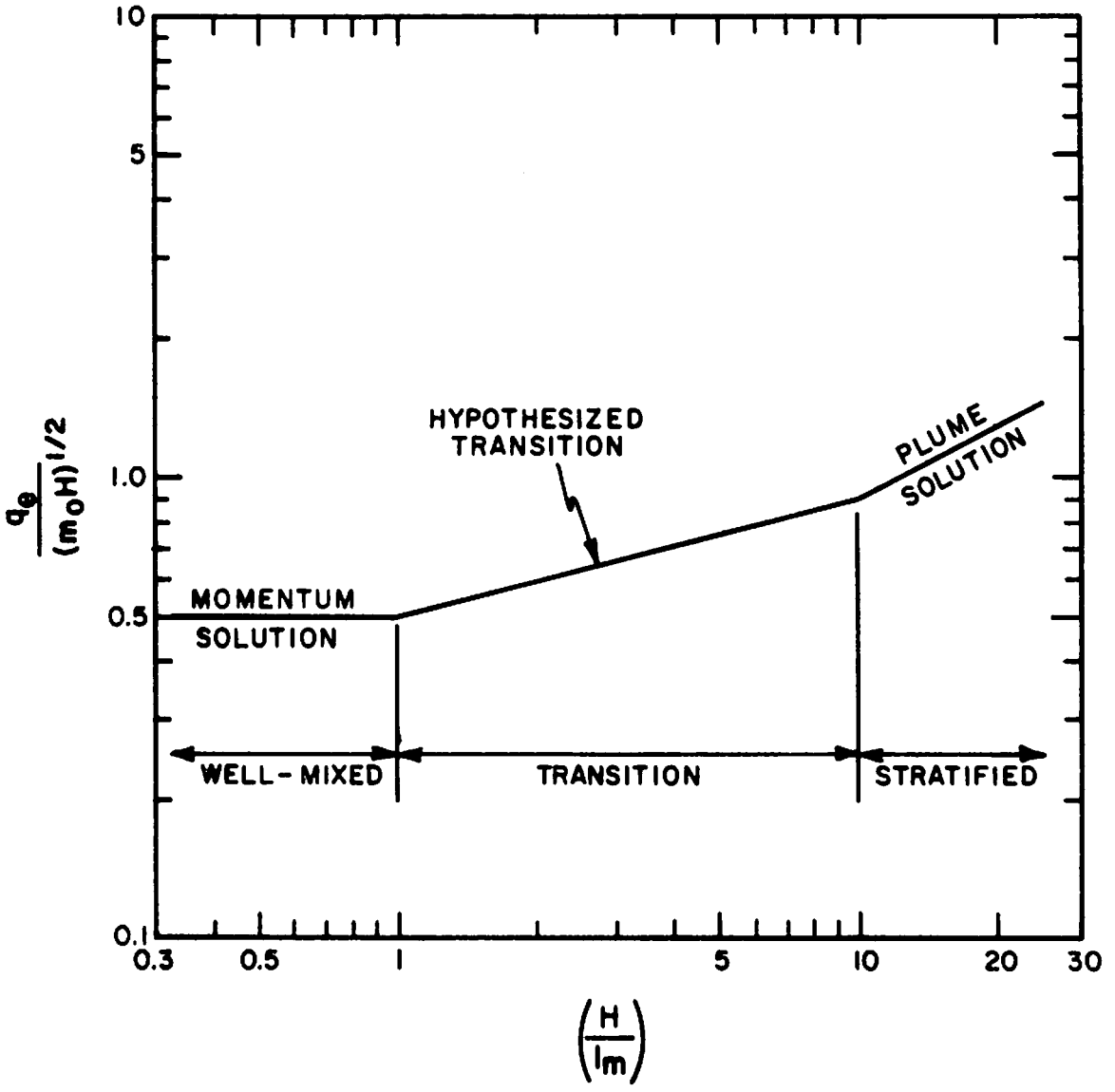

Figure 4.3 : Theoretical Solutions
for Entrained Diffuser Flow
Quiescent River Conditions

than zero are not shown since they would obscure the nature of the theory. The actual positions of the curves and the transitions are not fixed at this point. They are a function of the diffuser geometry and must be determined experimentally.

The coefficients of the momentum and the plume solutions, Equations (4.9), (4.10) and (4.13), are not necessarily applicable to the geometry of the Sequoyah diffuser. This problem is solved by introducing an experimentally determined coefficient, C_m, into Equations (4.9) and (4.10) so that they read

$$q_e/(m_o H)^{\frac{1}{2}} = C_m/\sqrt{2} \tag{4.14}$$

and

$$\frac{q_{em}}{(m_o H)^{1/2}} = C_m/2 \left[\frac{|V|}{b_o^{1/3}} \left(\frac{H}{\ell_m}\right)^{1/2} + \left(\frac{V^2 H}{b_o^{2/3} \ell_m} + 2 \text{ sign } (V)\right)^{1/2} \right] \tag{4.15}$$

and by introducing experimentally determined coefficient, C_b, to yield

$$q_e/(m_o H)^{\frac{1}{2}} = C_b \ (H/\ell_m)^{\frac{1}{2}}. \tag{4.16}$$

Figure 4.3 illustrates the nature of the quiescent solution and indicates the way the transition is handled. The transition solution is assumed to depend on H/ℓ_m in a way intermediate between Equations (4.14) and (4.16). The form chosen is

$$q_e/(m_o H)^{\frac{1}{2}} = C_t\ (H/\ell_m)^{\frac{1}{3}} \qquad (4.17)$$

where C_t is an experimentally determined coefficient.

A complete solution must include the behavior of the diffuser when $V/b_o^{1/3}$ is greater or less than zero. As stated previously, Equations (4.10) and (4.15) are valid for large values of $V/b_o^{1/3}$ regardless of the value of H/ℓ_m. For dimensional reasons Equation (4.15) is expected to be valid when $V/b_o^{1/3}$ is greater than o(1) or less than o(-1). When $V/b_o^{1/3}$ is greater than o(-1) and less than o(1) the solution is assumed to be a linear interpolation between the quiescent solution and Equation (4.15). Intead of o(-1) and o(1), values of -1.0 and 1.5 are used in the actual formulas (Table 2). The reason for this choice will be discussed in Chapter VI.

The final consideration is the value of H/ℓ_m below which the momentum solution is applicable and the value of H/ℓ_m above which the plume solution is applicable. These values are called t_m and t_b, respectively. In Figure 4.3 t_m is 1 and t_b is 10. The values of t_m and t_b are not independent of C_m, C_t and C_b. For instance, if C_m and C_t have been determined, t_m is fixed since the momentum solution and the transition solution must give the same answer when H/ℓ_m equals t_m.

The complete solution, except the values of the experimental coefficients, is presented in Table 2. In box 7 of Table 2 Equation (4.15) is modified so that entrained flow, Q_e, does not exceed the ambient river flow, Q_R. Q_{Rlim} in box 7 is defined as

$$\begin{aligned} Q_{Rlim} &= Q_R\ (H/\ell_m)/t_m && H/\ell_m \geq t_m \\ &= Q_R && H/\ell_m < t_m. \end{aligned} \qquad (4.18)$$

Table 2

SUMMARY OF ENTRAINMENT FORMULAE – Coflowing Diffuser

$\frac{V}{b_o^{1/3}}$	$< t_m$ MOMENTUM DOMINATED	$\frac{H}{l_m}$ $t_m - t_b$ TRANSITION	$> t_b$ BUOYANCY DOMINATED
< 0	① $\frac{q_e}{(m_o H)^{1/2}} = \begin{cases} \frac{C_m}{2}\left[M\left(\frac{H}{m_o}\right)^{1/2} + \left(\frac{V^2 H}{m_o} - 2\right)^{1/2}\right] & \text{if } \frac{V^2 H}{m_o} \geq 2 \\ \text{unsteady heat buildup} & \text{if } \frac{V^2 H}{m_o} < 2 \end{cases}$	② $\frac{q_e}{(m_o H)^{1/2}} = C_1\left(\frac{H}{l_m}\right)^{1/4} + \left(\frac{q_{e1}^*}{(m_o H)^{1/2}} - C_1\left(\frac{H}{l_m}\right)^{1/4}\right)\frac{M}{b_o^{1/3}}$ where $q_{e1}^* = q_e$ from ① evaluated $V = b_o^{1/3}$	③ $\frac{q_e}{(m_o H)^{1/2}} = C_b\left(\frac{H}{l_m}\right)^{1/2} + \left(\frac{q_{e1}^*}{(m_o H)^{1/2}} - C_b\left(\frac{H}{l_m}\right)^{1/2}\right)\frac{M}{b_o^{1/3}}$ where $q_{e1}^* = q_e$ from ① evaluated at $V = b_o^{1/3}$
0	④ $\frac{q_e}{(m_o H)^{1/2}} = \frac{C_m}{\sqrt{2}}$ unsteady heat buildup	⑤ $\frac{q_e}{(m_o H)^{1/2}} = C_1\left(\frac{H}{l_m}\right)^{1/4}$ possible unsteady heat buildup as $\frac{H}{l_m} \to 1$	⑥ $\frac{q_e}{(m_o H)^{1/2}} = C_b\left(\frac{H}{l_m}\right)^{1/2}$
$0 - 1.5$	⑦ $\frac{q_e}{(m_o H)^{1/2}} = \begin{cases} \frac{C_m}{2}\left[V\left(\frac{H}{m_o}\right)^{1/2} + \left(\frac{V^2 H}{m_o} + 2\right)^{1/2}\right] & \text{if } Q_e < Q_{R_{lim}} \\ \frac{Q_R / L}{(m_o)^{1/2}} & \text{if } Q_e \geq Q_{R_{lim}} \end{cases}$	⑧ $\frac{q_e}{(m_o H)^{1/2}} = C_1\left(\frac{H}{l_m}\right)^{1/4} + \left(\frac{q_{e7}^*}{(m_o H)^{1/2}} - C_1\left(\frac{H}{l_m}\right)^{1/4}\right)\frac{V}{1.5 b_o^{1/3}}$ where $q_{e7}^* = q_e$ from ⑦ evaluated at $V = 1.5\, b_o^{1/3}$	⑨ $\frac{q_e}{(m_o H)^{1/2}} = C_b\left(\frac{H}{l_m}\right)^{1/2} + \left(\frac{q_{e7}^*}{(m_o H)^{1/2}} - C_b\left(\frac{H}{l_m}\right)^{1/2}\right)\frac{V}{1.5 b_o^{1/3}}$ where $q_{e7}^* = q_e$ from 7 at $V = 1.5\, b_o^{1/3}$
> 1.5	⑩ same as ⑦	⑪ same as ⑦	⑫ same as ⑦

V. PHYSICAL MODEL STUDY

The purpose of the model study was to evaluate the performance of the diffuser over a wide range of variables and to determine the experimental coefficients which give the best fit of data to theory. Similitude requirements for the physical model study are discussed in the following section. In subsequent sections descriptions of the model, test procedure and data reduction are given. Analysis of the data will be given in the next chapter. Except where the context indicates otherwise, all quantities are given in field values to facilitate understanding of the conditions tested.

Similitude Requirements

The similitude requirements governing the modeling of buoyant discharges can be derived from the basic hydrodynamic and thermodynamic equations governing the flow field (Reference 7). The following requirements are found to be important in achieving similitude in the near field region:

1. The model should accurately reproduce the field densimetric Froude number, F', defined as

$$F' = \frac{u}{\left(g \frac{\rho - \rho_o}{\rho_o} \ell\right)^{1/2}} \tag{5.1}$$

where

u = characteristic velocity

ℓ = characteristic length.

Denoting the ratio between field and model values by the subscript r, this requirement is equivalent to

$$U_r = ((\rho_a-\rho_o)/\rho_a)_r^{\frac{1}{2}}\, g_r^{\frac{1}{2}}\, \ell_r^{\frac{1}{2}} \qquad (5.2)$$

In this study, $((\rho_a - \rho_o)/\rho_a)_r^{\frac{1}{2}}$ is set to unity and g_r is unity, identically. Under these conditions Equation (5.2) states that the velocity ratio is proportional to the square root of the length ratio.

2. The model should be geometrically undistorted, i.e. the length ratio, ℓ_r, should apply in all directions. Since near-field mixing responds primarily to the overall geometry, including the location of river banks, river depth and major underwater flow obstructions, the riverbed is modeled as a rectangular channel. The slight bend of the river (Figure 2.1) and the difference between a rectangular channel and the actual channel (Figure 2.2) are considered unimportant to model similitude. The underwater dam was modeled.

3. The exit Reynolds number of each port in the model, R_{pm}, must be large enough to ensure turbulent conditions in the jet mixing zone. The port Reynolds number is defined as

$$R_{pm} = U_o D_o/\nu \qquad (5.3)$$

where

U_o = exit velocity of the model discharge

D_o = diameter of model port

and

ν = the kinematic viscosity.

Laboratory experiments have shown that R_{pm} greater than about 1500 will ensure a fully turbulent jet whose mixing characteristics are independent of R_{pm} (Reference 8). The condition,

$$R_{pm} > 1500, \tag{5.4}$$

is a constraint on the model scale selected and the number of ports which may be included in the model. In the field port Reynolds numbers are always much larger than 1500.

4. The essential discharge characteristics of the diffuser must be preserved. The actual diffuser at Sequoyah Nuclear Plant has alternating columns of eight and nine two-inch diameter holes over the whole length, Figure 3.1. Exact modeling of individual ports would violate Equation (5.4). The overall mixing characteristics of the diffuser may be modeled correctly by using a row of evenly spaced ports whose total scaled area is equal to that of the original diffuser. This widely used concept is described by Cederwall (Reference 9). The total number of ports must be large enough so that the discrete nature of the ports does not affect overall diffuser performance. Reference 10 indicates that this number may be as small as six as long as interest is directed at least one diffuser length downstream. In the present study 13 ports were used for each leg. This value of n allows discharge flows as small as 475 ft^3/sec per diffuser leg to be modeled at the scale chosen.

Because the diffuser extends most of the distance across the main channel, it was necessary to model the full 900 foot width of the main channel. The available discharge flume was 10 feet wide. These

dimensions require a 1:90 scale model. The relatively shallow overbank areas were not modeled; this deletion is not considered serious since the overbank areas may not be able to effectively contribute to diffuser induced mixing.

Description of the Physical Model

All tests were run in the 10 ft x 70 ft (3 m x 21 m) thermal discharge flume at the Engineering Laboratory of TVA's Water Systems Development Branch. A schematic of the model flume setup is shown in Figure 5.1. This flume allowed a 6300 ft (1900 m) section of the river to be modeled. Except for a 20 ft (6.1 m) section of plexiglas along the left side, the entire flume is insulated with one-inch thick styrofoam sheets. The water in the flume is delivered to the upstream end of the flume through an adjustable mainfold in order to insure an even flow distribution. Just downstream of the manifold is a 6 in (15 cm) thick trough filled with glass spheres placed across the full width and depth of the flume. The trough further distributes the flow and damps out waves caused by the manifold. The rate of flow in the flume is measured by an orifice plate located between the manifold and a constant head tank.

Models of the diffuser and the underwater dam are attached to the false floor of the flume. Each diffuser port is fed individually via tygon tubing from a circular discharge manifold in order to ensure an even flow distribution. The discharge flow rate is measured by either a rotameter or an elbow meter depending on the flow rate required. Water at the desired temperature is obtained from a mixing valve-controller which supplies water at constant temperature and

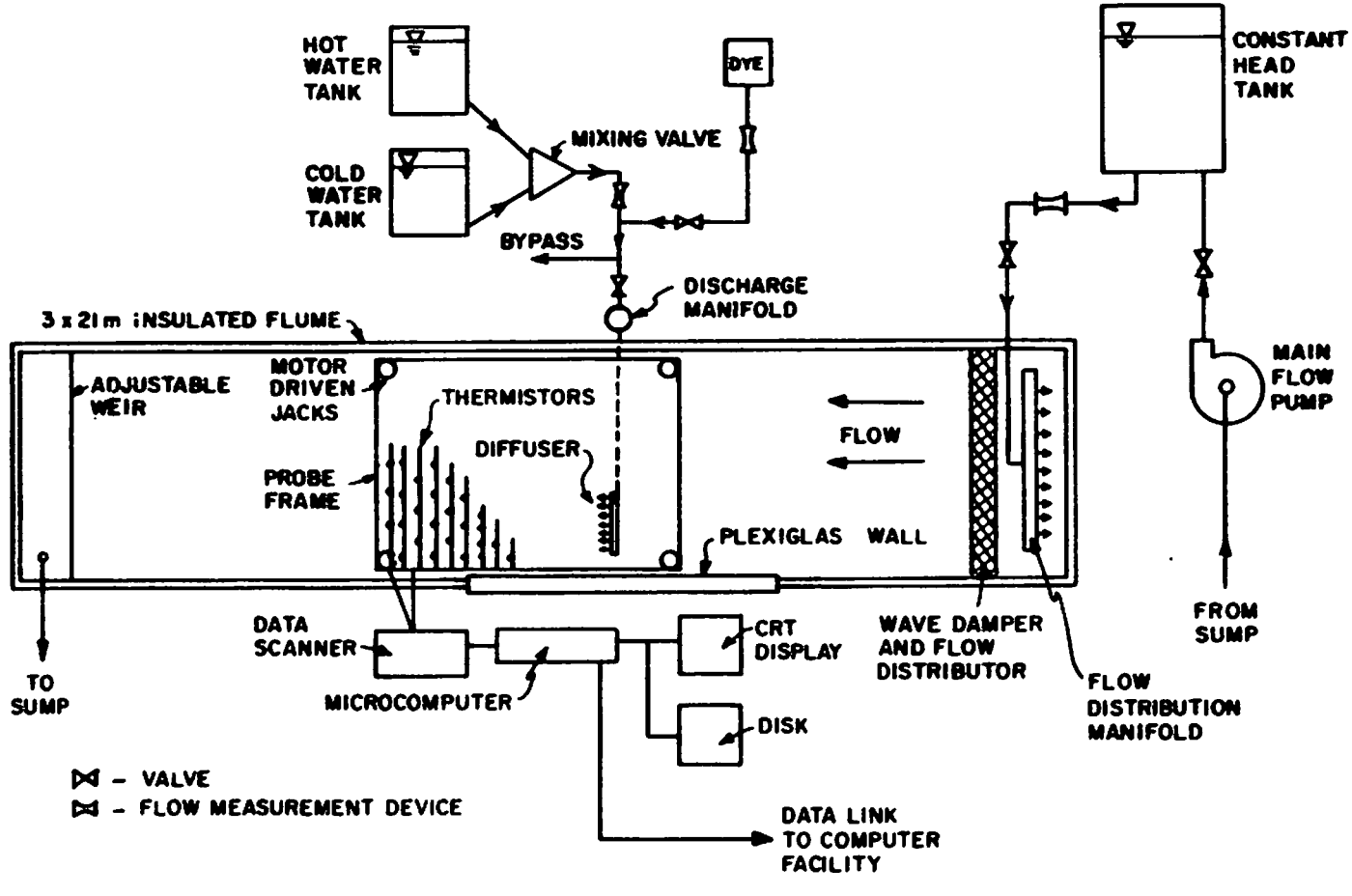

Figure 5.1 : Schematic Layout of Physical Model (not to scale)

pressure. Hot and cold water are supplied to the mixing valve-controller from pressure matched sources. A gravity-feed dye bottle can be used to inject dye into the discharge line for flow visualization purposes.

Instrumentation

One hundred thermistors were used to measure temperatures in the flume and in the discharge manifold. Ninety-three thermistors were mounted at one level on the 10 ft x 21.5 ft (3 m x 6.6 m) metal frame shown in Figure 5.1. The frame rides on carriage rails and may be moved the length of the flume. Motor driven jacks at the four corners of the probe frame enable vertical movement of the thermistor array, allowing temperature maps to be made at any desired level. Thermistor locations are shown in Figure 5.2. In addition to the probe frame thermistor array, four thermistors were mounted vertically above the underwater dam at a position which corresponds to the end of the downstream leg of the diffuser. In order to give an indication of when model boundary effects were becoming important, one thermistor was mounted on the downstream weir and one thermistor was mounted on the wave damper.

A microcomputer controlled data acquistion system reads the probe temperatures in approximately six seconds and then simultaneously stores the values on a floppy disk and displays them on the system CRT (Figure 5.1). The microcomputer also controls and records the vertical position of the probe frame, and controls the frequency at which temperature scans are made. Final data reduction takes place on a larger computer via a high speed data transmission link.

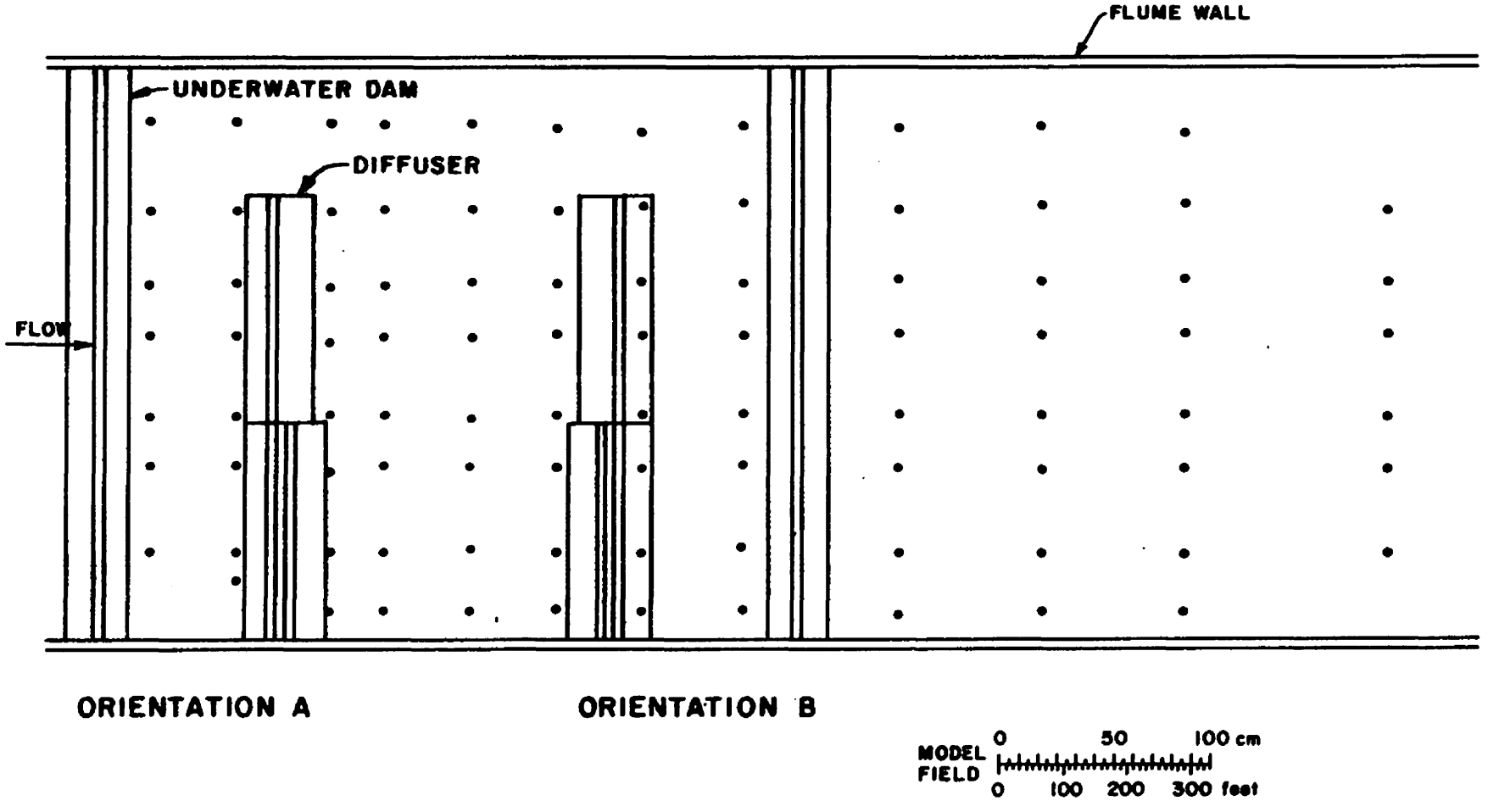

Figure 5.2 : Location of Thermistors on Probe Frame and Orientations A and B of the Diffuser and Underwater Dam

Model Test Program

The model test program was designed to test the diffuser under a sufficiently wide range of discharge flow rates, discharge temperatures and ambient flow rates to allow prediction of diffuser performance under all reasonable conditions which might be of concern. Very high river flows were not studied since dilutions will always be adequate. Four river velocities were tested: -0.10, 0, 0.29 and 0.58 fps (-2.9, 0, 8.7 and 17.5 cm/s), which correspond to Tennessee River flows of about -5000, 0, 15000, and 30000 cfs (-142, 0, 425 and 850 m^3/s). Diffuser discharge rates of 475, 875 and 1250 cfs (13, 25 and 35 m^3/s) per leg were tested for both legs operating and for the upstream leg only operating. Discharge temperature rises of 10, 20 and 30°F (5.6, 11, 17°C) above ambient were tested. The results of the physical model study combined with the theory presented previously will enable predictions of dilution for conditions not explicitly tested here.

Data Acquisition and Reduction Procedure

The zone of diffuser induced mixing may be considered to extend from the diffuser to one or two diffuser lengths downstream. Beyond this region temperature decay is also influenced by processes other than diffuser induced mixing, such as surface heat loss, natural turbulence and interfacial shear between the buoyant upper and cooler lower layers. The undistorted physical model does not reproduce these processes accurately. In order to consistently and objectively identify the dilution characteristics of the diffuser induced mixing region, the following data acquisition and reduction procedure was used:

1. Temperature readings were made near the surface (5 foot depth) and near the bottom (15 foot elevation above the bottom) prior to the start of each test. This defined ambient conditions and verified that no stratification was present in the flume.

2. During the test, temperature scans at the 53, 45, 30 and 15 feet (16.2, 13.7, 9.1 and 4.6 m) levels above the bottom were taken about every five minutes. The 53 foot level corresponds to five feet below the surface, the depth at which environmental standards specify temperature measurements be made.

3. For each test, the average of the temperature rises for a set of probes one diffuser length long located along a line parallel to the diffuser about one diffuser length downstream of the diffuser was computed. These probes were those directly downstream from the diffuser. Analysis of temperature maps from the complete thermistor array indicated that this choice of probes gave a temperature which was representative of the mixing achieved by the diffuser.

4. With only one exception, the highest average diffuser induced mixed temperature rise occurred at the 53 foot level. For this reason the mixed temperatures at the 53 foot level were taken as the measure of diffuser induced mixed temperature.

5. For each test, the temperature scans at the 5 foot depth which occurred between about ten and thirty minutes into the test were examined. Generally, the mixed temperatures measured at 20 to 25 minutes into the test were used since steady state conditions in the near-field had been achieved but model boundary effects were not yet important.

VI. RESULTS

In this chapter the results of the physical model study are presented and discussed. A qualitative discussion of the generally observed features of diffuser performance is given first. The second section presents a quantitative examination of the results and the recommended form of the theory for this particular diffuser. A summary of the test conditions and the observed results is presented in the Appendix.

General Features

As discussed in Chapter IV a heated effluent will tend to stratify. Figure 6.1 shows vertical temperature profiles of induced temperature rise representative of the extreme cases studied; note that all cases show some stratification. Figure 6.1a shows the very strong stratification which occurs for a high buoyancy discharge under zero river flow conditions. In contrast, Figure 6.1d shows the mild stratification which results from a high momentum, high river flow case. Figures 6.1b and 6.1c show cases in which both momentum and buoyancy play important roles. Figure 6.1b shows a high momentum discharge, zero river flow case. As should be expected for a high momentum discharge, the flowaway layer in Figure 6.1b is vertically well mixed. Figure 6.1c shows a high buoyancy discharge, high river flow case; the stratification is intermediate between those of Figures 6.1a and 6.1d. Under zero river flow conditions the warm water discharged by the diffuser mixes with cold water and then flows away both upstream and downstream on the surface. As a result cold water must

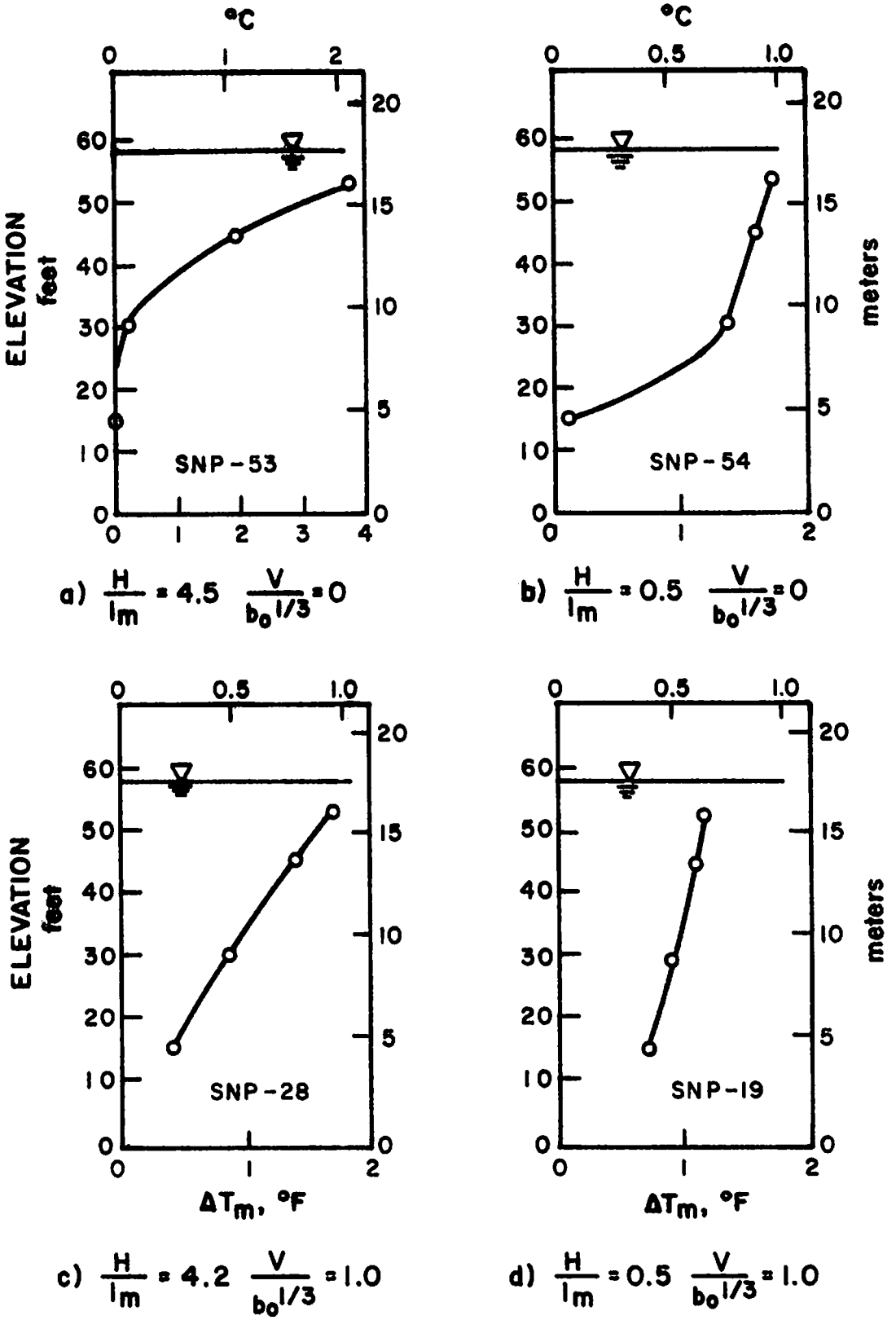

Figure 6.1 : Typical Vertical Temperature Profiles

flow back toward the diffuser along the bottom of the channel. Figures 6.1a and 6.1b show evidence of this effect.

In this model study no attempt was made to model the unsteady effects. In every case our attention was on the steady state; however, certain unsteady effects in the model must be considered in evaluating diffuser performance. Figure 6.2a shows the measured induced temperature rise as it varies with time for a normal coflowing situation. This figure illustrates the rapid temperature rise and steady plateau found under normal coflowing conditions. Figure 6.2b illustrates the features found when the river flow is zero; the temperature rises quickly to a plateau and then after about twenty minutes begins to rise again. The second temperature rise is the result of the limited size of the flume; as the cool water in the flume gets used up in mixing with the hot discharge, less water is available for cooling. Since the reservoir is much larger than that part modeled in this study, the three hour (field time) plateau which corresponds to the twenty minute plateau observed in this example is probably much shorter than would be observed in the field; however, it is not possible to accurately predict the duration of the plateau region on the basis of this study. Since temperatures measured during the unsteady temperature buildup are a result of the finite flume size and not a measure of diffuser performance the data must be analyzed accordingly.

A small number of runs were redone with the underwater dam removed (see Appendix). No measurable differences in achieved dilution were found when these runs were compared with the previous runs with the dam.

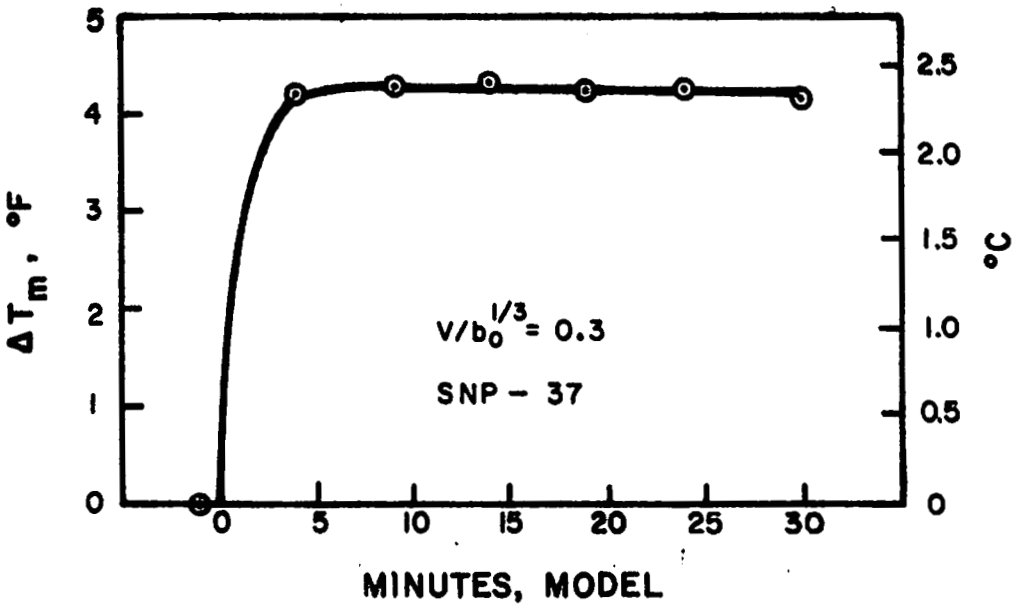

a)

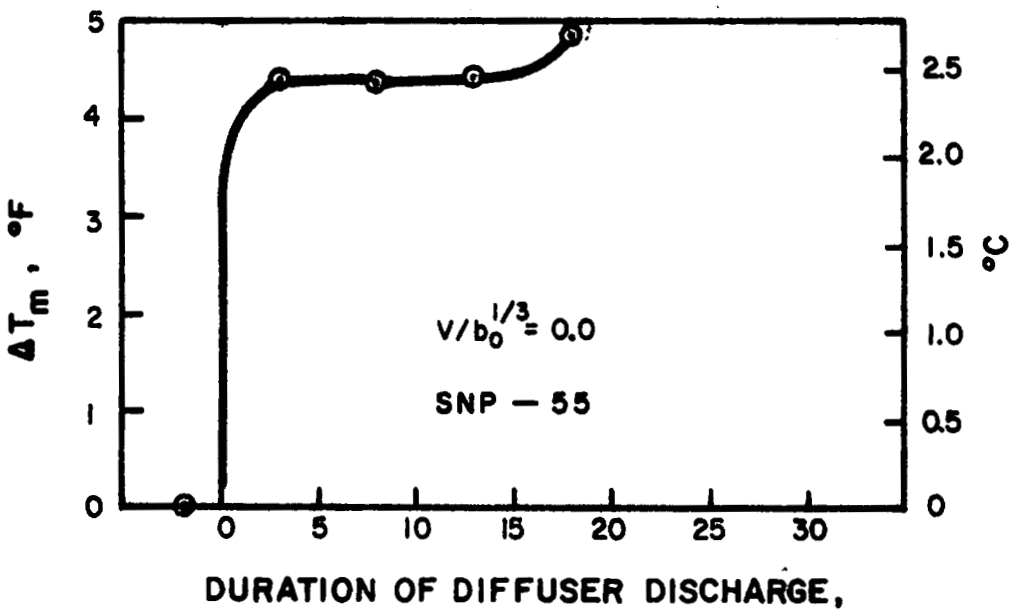

b)

Figure 6.2 : Examples of Time Variation of Measured Temperature Rise.

Comparison to Theory

The primary result desired of this physical model study is the induced temperature rise at the five-foot depth since that is where environmental standards are applicable. In this section, the measured temperature rises at the five-foot depth are represented within the theoretical framework.

As discussed in Chapter IV, for any particular diffuser geometry the diffuser induced entrainment flow can be expressed as in Table 2. The parameters which can be adjusted to specialize this theory to a particular diffuser are C_m, C_t, C_b, t_m and t_b. The best values of these parameters for the upstream leg only and for both legs together are given in Table 3. The criterion used to define the best values is that the sum of the mean error and the standard deviation of the error between the measured and predicted temperature rises be zero. This criterion is slightly conservative since the induced temperature rises will be underpredicted by the standard deviation on the average.

Table 3: Values of the Experimentally Determined Coefficients

	C_m	C_t	C_b	t_m	t_b
Both Legs	0.40	0.40	0.22	0.24	10.
Upstream Leg	0.42	0.52	0.29	0.11	10.

As discussed in Chapter IV, when $V/b_o^{1/3}$ is between o(-1) and o(1) the formulas used are linear interpolations between the appropriate quiescent solution and Equation (4.15). The quantity of data from this study was not sufficient to accurately identify the best transition values of $V/b_o^{1/3}$. Following Reference 3, the transition values were originally set to -1.0 and 1.0. Examination of the data indicated that a value of 1.5 instead of 1.0 would fit the data better. This proved true but the improvement was not sufficient to justify further effort. As shown in Table 2, the values used in this report are -1.0 and 1.5.

Figures 6.3 and 6.4 show non-dimensional plots of data and theoretical projections for the single upstream diffuser leg and for both diffuser legs, respectively. These plots show fairly good agreement between the data and the theory. Generally, the theory under predicts dilution, especially at higher values of $V/b_o^{1/3}$. For data points with $V/b_o^{1/3} \sim 0.5$ the theory appears to over predict dilution somewhat.

These discrepancies are probably due to the formulation of the theory in the transition regime. The quiescent transition formula is merely an hypothesized transition between the two known quiescent solutions. The formula for values of $V/v_o^{1/3}$ less than o(1) are perhaps even more uncertain since they are simple linear transitions between the quiescent solutions and the high river momentum solution; the actual behavior of the transition mixing is likely much more complex. In spite of the incomplete success of the theory, the practical results are quite acceptable.

Figures 6.5 and 6.6 show comparisons between theory and measured data points. Figure 6.5 shows a comparison for the upstream

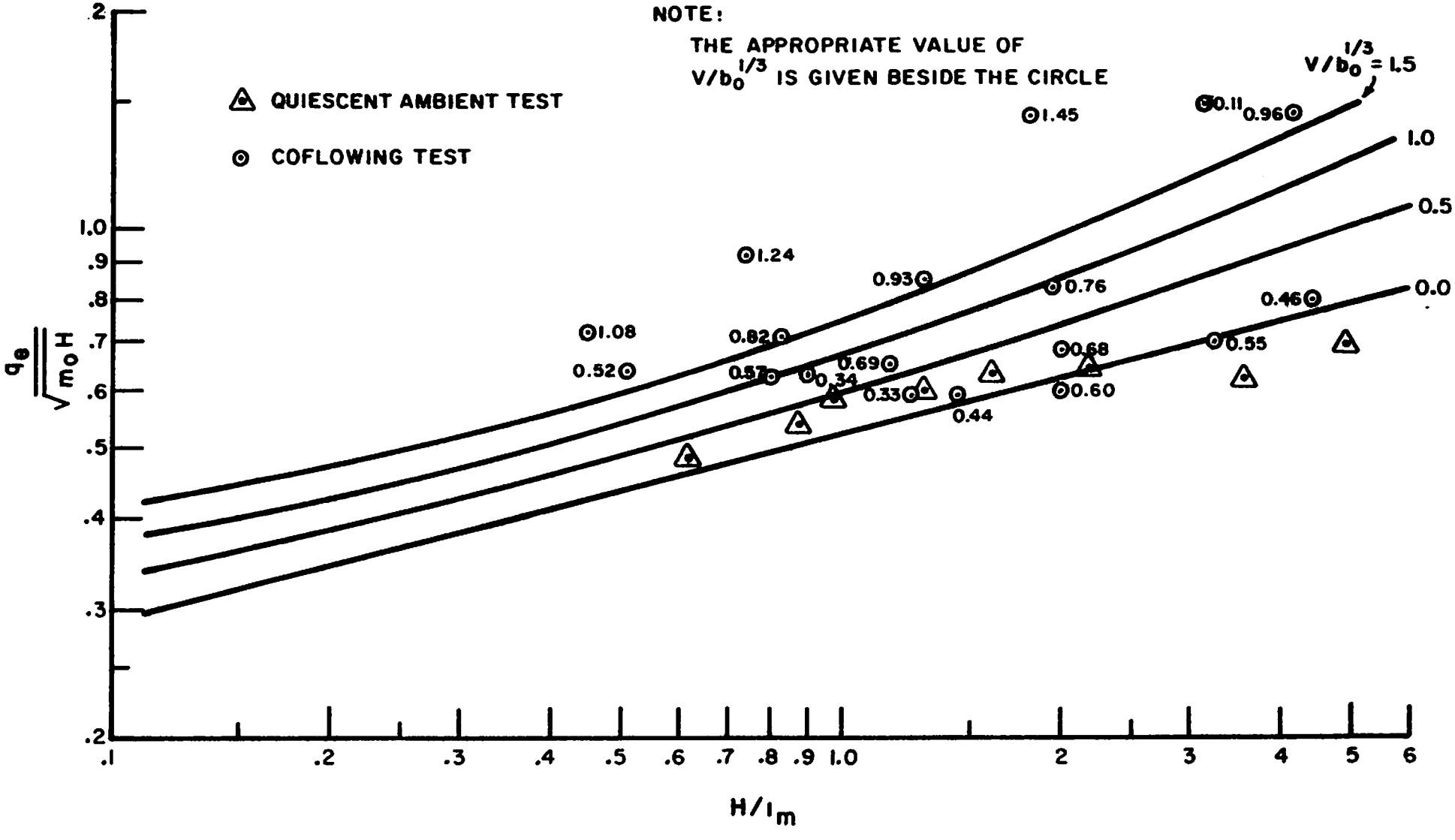

Figure 6.3: Comparison of Theory and Data for Upstream Diffuser Leg Only

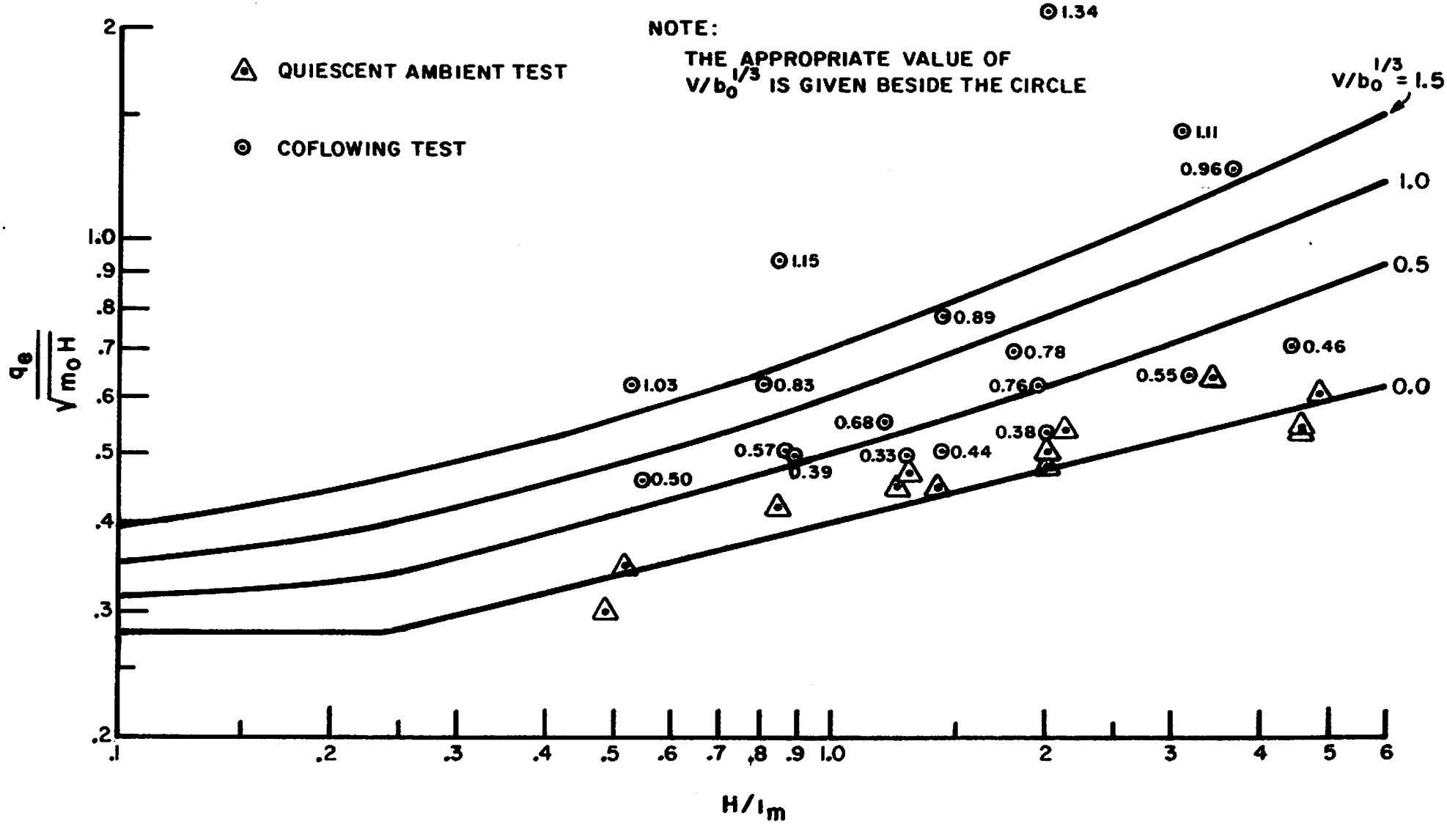

Figure 6.4: Comparison of Theory and Data for Both Diffuser Legs Together

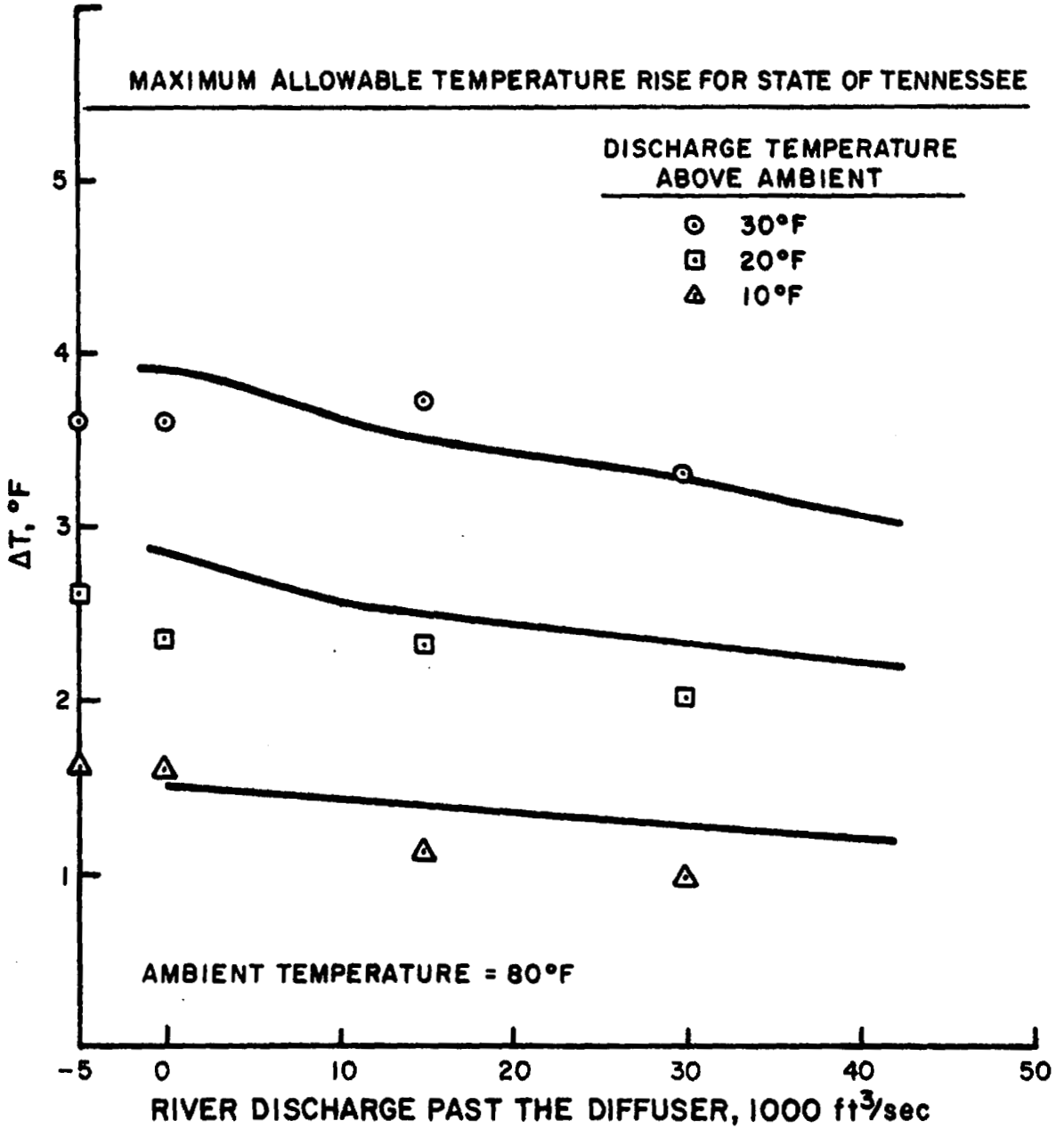

Figure 6.5: Measured and Calculated Induced Temperature Rise at Maximum Upstream Leg Discharge Rate, 1250 cfs

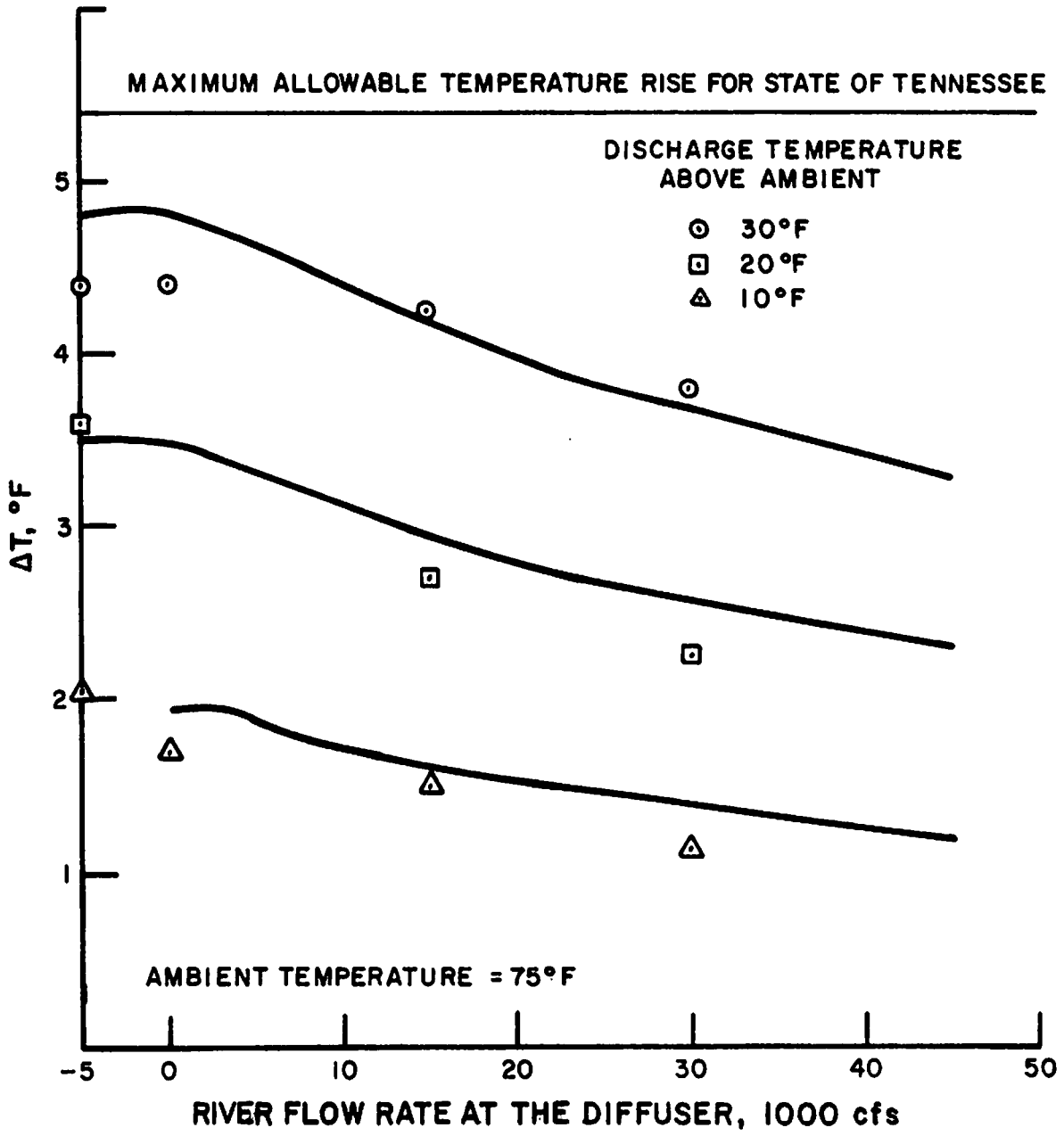

Figure 6.6: Measured and Calculated Induced Temperature Rise at Maximum Diffuser Discharge Rate, 2500 cfs

leg at the maximum discharge rate. The solid lines show the predictions of the theory for discharges at 10, 20 and 30°F (5.6, 11 and 17°C) above the ambient temperature of 80°F (27°C). Figure 6.6 shows the same comparisons except that both diffuser legs are operating together at maximum discharge rate and that the predictions of the theory are based on a 75°F (24°C) ambient temperature. From the practical standpoint the match between data and the theory are completely adequate for the predicting diffuser induced temperature rise with confidence. For low and reverse river flow conditions these figures and the prediction of the theory should be interpreted carefully. As mentioned earlier when the ambient water is quiescent the supply of cool water to mix with the warm diffuser discharge is limited and as that supply is depleted the mixed water temperature will rise until it reaches the temperature of the discharge or until other heat loss mechanisms become important.

Conclusions

The results presented in this chapter have shown to be consistent with the theory of Chapter IV. With inclusion of the experimentally determined coefficients the theory predicts mixed temperature rises which are slightly conservative. Due to the depletion of cool ambient water under low flow conditions the mixed temperature will exceed the predictions of the theory if the discharge or ambient flow conditions continue too long.

The mathematical form of the theory is shown in detail in Table 2. The experimentally determined coefficients are given in Table 3.

REFERENCES

1. Johnson, B. E. and W. R. Waldrop, "The Natural Thermal Regime of Chickamauga Reservoir in the Vicinity of Sequoyah Nuclear Plant," TVA Division of Water Management, Water Systems Development Branch, Report No. WM28-1-45-100, February 1978.

2. Ungate, C. D. and K. A. Howerton, "Effect of Sequoyah Nuclear Plant Discharges on Chickamauga Lake Water Temperatures," TVA Division of Water Management, Water Systems Development Branch, Report No. WM28-1-45-101, April 1978.

3. Almquist, C. W., "Submerged Multiport Diffuser Analysis and Design for Hartsville Nuclear Plant," TVA Division of Water Management, Water Systems Development Branch, Report No. WM28-1-89-100, September 1978.

4. Adams, E. E., "Submerged Multiport Diffusers in Shallow Water with Current," Massachusetts Institute of Technology, Department of Civil Engineering, Master's Thesis, June 1972.

5. Rouse, H., C. S. Yih and H. W. Humphreys, "Gravitational Convection from a Boundary Source," Tellus, Vol. 14, 1952.

6. Cederwall, K., "Gross Parameter Solution of Jets and Plumes," Journal of the Hydraulics Division, ASCE, Vol. 101, No. HY5, May 1975.

7. Stolzenbach, K. D., and D.R.F. Harleman, "An Analytical and Experimental Investigation of Surface Discharges in Shallow Water," Massachusetts Institute of Technology, Ralph M. Parsons Laboratory for Water Resources and Hydrodynamics, Report No. 169, March 1973.

8. Ungate, C. D., et al, "Mixing of Submerged Turbulent Jets at Low Reynolds Number," Massachusetts Institute of Technology, Ralph M. Parsons Laboratory for Water Resources and Hydrodynamics, Report No. 197, February 1975.

9. Cederwell, K., "Buoyant Slot Jets into Stagnant or Flowing Environments," California Institute of Technology, W. M. Keck Laboratory for Hydraulics and Water Resources, Report No. KH-R-25, 1970.

10. Almquist, C. W., and C. D. Ungate, "Submerged Multiport Diffuser Design for Bellefonte Nuclear Plant," TVA Division of Water Management, Water Systems Development Branch, Report No. WM28-1-88-003 (Formerly 81-13), September 1977.

APPENDIX

Summary of Test Conditions

This appendix contains a summary of conditions tested in the physical model study. The following parameters (defined in Chapter IV) were held constant:

W = 900 ft (274.3 m)

H = 58 ft (17.7 m) field values

h = 14.7 ft (4.5 m)

α = 33°

The following key applies to the summary of runs on succeeding pages (field values):

Number of diffuser legs, NL

1 - upstream leg only, 350 ft (106.7 m)

2 - both legs, 700 ft (213.4 m)

Discharge flow rate per leg, $Q_{o\ell}$

1 - 475 cfs (13.5 m^3/s)

2 - 875 cfs (24.8 m^3/s)

3 - 1250 cfs (35.4 m^3/s)

4 - 950 cfs (26.9 m^3/s)

Initial Temperature Rises, ΔT_o

1 - 10°F (5.6°C)

2 - 20°F (11.1°C)

3 - 30°F (16.7°C)

River Velocities, V

1 - .58 fps (0.18 m/s)

2 - .29 fps (0.09 m/s)

3 - 0.0 fps (0 m/s)

4 - -.10 fps (-0.03 m/s)

Runs which were lost or some way flawed are marked by a † in the ΔT_m column.

Runs with an * after the run number were performed with underwater dam removed.

Run Summary

Run #	NL	Q	T_o	V	ΔT_m (measured temperature rise °F)
SNP - 1					†
2	2	1	1	1	0.4
3	2	1	2	1	1.0
4	1	2	3	1	2.7
5	1	1	1	1	0.5
6	1	1	2	1	1.0
7	1	1	3	2	2.8
8	1	1	2	2	2.0
9	1	1	1	2	1.1
10	1	2	3	2	3.5
11	1	2	2	2	2.4
12	1	2	1	2	1.2
13	1	3	3	2	3.7
14	1	3	2	2	2.3
15	1	3	1	2	1.1
16	2	2	3	1	3.9
17	2	2	2	1	1.9
18	2	3	3	1	3.8
19	2	3	1	1	1.1
20	2	2	1	1	0.8
21	2	3	2	1	2.2
22	1	1	3	1	1.6
23	1	2	2	1	1.6
24	1	2	1	1	0.7
25	1	3	3	1	3.3
26	1	3	2	1	2.0
27	1	3	1	1	0.9
28	2	2	3	1	1.8
29	2	2	3	2	3.1
30	2	2	2	2	2.2
31	2	1	1	2	1.0
32					†
33	2	2	3	2	3.9
34	2	2	1	2	1.4
35	2	2	2	2	2.7
36	2	3	1	2	1.5
37	2	3	3	2	4.3
38	2	3	2	2	2.7

Runs 39 through 52 were not analyzed because it was found that the model boundaries had an unnecessarily large effect. Certain changes were made and the conditions tested in runs 39 through 52 were repeated in subsequent runs.

53	2	1	3	3	3.8
54	2	3	1	3	1.7
55	2	3	3	3	4.4
56*	2	3	3	2	4.0
57*	2	1	3	2	3.0
58					†
59*	2	1	3	3	4.1
60	2	1	3	3	3.8
61	2	2	3	3	4.1
62	2	2	3	3	4.3
63	2	3	3	3	4.4
64					†
65	2	3	1	3	1.7
66	2	2	2	3	2.8
67	2	2	1	3	1.5
68	2	1	2	3	2.6
69	2	1	1	3	1.4
70	2	1	3	3	3.5
71	2	1	2	4	2.5
72	2	1	1	4	1.3
73	2	2	3	4	4.0
74	2	2	2	4	2.7
75	2	2	1	4	1.6
76	2	3	3	4	4.4
77	2	3	2	4	3.6
78	2	3	1	4	2.1
79	1	3	3	4	3.6
80	1	3	2	4	2.6
81	1	3	1	4	1.6
82	1	2	3	4	3.5
83	1	2	2	4	2.3
84	1	2	1	4	1.2
85	1	1	3	4	2.2
86	1	1	2	4	2.2
87	1	1	1	4	1.1
88	1	1	3	3	3.2
89	1	1	2	3	2.3
90	1	1	1	3	1.2
91	1	2	3	3	3.9
92	1	2	2	3	2.4
93					†
94	1	3	3	3	3.6
95	1	3	2	3	2.3
96	1	3	1	3	1.6
97	1	2	1	3	1.1
98	1	4	3	4	3.7
99*	1	3	3	4	3.7
100*	1	3	3	3	3.6
101					†
102*	2	3	2	4	4.6